Journal of Sound and Vibration (2001) **245**(5), 845–875
doi:10.1006/jsvi.2001.3610, available online at http://www.idealibrary.com on IDEAL®

A WAVELET-GALERKIN PROCEDURE TO INVESTIGATE TIME-PERIODIC SYSTEMS: TRANSIENT VIBRATION AND STABILITY ANALYSIS†

S. PERNOT AND C.-H. LAMARQUE

Ecole Nationale des Travaux Publics de l'Etat, LGM/DGCB—URA CNRS 1652, 1, *rue Maurice Audin*, 69518 *Vaulx-en-Velin Cedex, France. E-mail: stephane.pernot@entpe.fr*

(*Received* 29 *November* 1999, *and in final form* 5 *January* 2001)

A wavelet-Galerkin procedure is introduced in order to obtain transient and periodic solutions of multi-degree-of-freedom (d.o.f.s) dynamical systems with time-periodic coefficients. Numerical comparisons, achieved with a Runge–Kutta method, emphasize that the wavelet-based procedure is reliable even in the case of problems involving both smooth or non-smooth parametric excitations and a relatively large number of degrees of freedom. The procedure is then applied to study the vibrations of some theoretical parametrically excited systems. Since problems of stability analysis of non-linear systems are often reduced after linearization to problems involving linear differential systems with time-varying coefficients, the method is shown to be effective for the computation of the Floquet exponents that characterize stable/unstable parameters areas and consequently allows estimators for stability/instability levels to be provided. Stability diagrams of some theoretical examples including a single-degree-of-freedom Mathieu oscillator and a two-degree-of-freedom parametrically excited system, illustrate the relevance of the method. Finally, future studies are outlined for the extension of the wavelet method to the non-linear case.

1. INTRODUCTION

In this paper, linear differential systems with T-periodic time-varying coefficients which are excited by an external force are investigated. The aim is first to describe an efficient wavelet-based procedure which allows transient solutions to such problems with any general time-varying functions to be computed (further developments will then extend the method to the stationary case dealing with periodic orbits). The procedure is then numerically validated using a few mathematical examples exhibiting various *a priori* difficulties. The motivation for such choices is to highlight the robustness of the wavelet-based method rather than studying actual mechanical systems. Nevertheless, this introduction is intended to explain why searching transient or stationary responses of dynamical systems is interesting and to highlight the state-of-art of linear differential systems with time-varying coefficients and especially its applications in the framework of mechanics and non-linear dynamics. Focusing investigations either on the study of small amplitude vibrations of mechanical systems with varying stiffness (see mechanical instances

†Some of the material in this paper was presented at the ASME Design Engineering Technical Conferences DETC'99, 17th Biennal Conference on Mechanical Vibration and Noise, Las Vegas, U.S.A., September 12–16th 1999.

0022-460X/01/350845 + 31 $35.00/0

thoroughly depicted in the book of Nayfeh [1]) or the stability analysis of non-linear systems, investigations often consist in finding periodic solutions. In the non-linear case, the system is linearized around a known periodic solution thanks to a perturbation technique so that a linear differential system with periodic time-varying coefficients is obtained. By linearization, the non-linear case is also equivalent to the study of the free oscillations of a linear differential system with time-varying coefficients. Summing up, the problem of interest is, on the one hand, strongly related to parametrically excited systems (eventually involving gyroscopic components) and, on the other hand, linked to the important question of (linearized) stability of smooth non-linear dynamical systems.

Searching periodic orbits of smooth linear systems governed by ordinary differential equations with time-varying coefficients can also be formulated using the following approach:

- Theoretical approach: linear differential systems and Floquet theory.
- Approximate computational approach using analytical methods.
- Approximate computational approach using numerical methods.

Though the theoretical framework of linear differential systems with time-varying coefficients is well known, and the mathematical background may be found in many references (see references [1, 2]), mathematical solutions are extremely difficult to compute from a practical point of view. The problem of searching for periodic solutions may be solved by building, for instance, a Poincaré map of the dynamic, reducing the problem to a theoretically questionable linear system of algebraic equations.

Analytical methods have been used extensively to compute approximate periodic solutions of non-linear differential systems. When linearizing these systems in the neighbourhood of the previously obtained orbits, stability is then investigated thanks to a similar analytical method. It is noticeable that many definitions exist to depict stability [3], one of the most important being the definition of linearized stability. Basically, analytical methods are very important to study vibrations and questions of stability [4]. Numerous analytical methods are introduced in references [5, 6] and many monographs which can be found in the literature are quoted below. Among analytical methods, normal form method developments are described in references [7–10] for the theoretical framework and in references [11–14] for practical calculations; in reference [9] Floquet theory is developed in the frame of normal form. In reference [13], Smith introduces a peculiar normal form theory, using a vector space of time-varying coefficients; reduction of smooth non-linear differential systems to linear systems is achieved here according to this vector space and not only to a scalar field. This approach is interesting whether or not time-varying components belong to the same vector space whose dimension is small enough to allow practical computations. Numerous other analytical methods are also commonly used such as perturbation methods [15], asymptotic methods [16], multiple scales methods [1], averaging methods or harmonic balance methods [17]. In reference [18], relations between normal forms and averaging are reported.

Standard parametrically excited systems refer to the well-known Mathieu and Hill equations issued from the stability analysis of a column (see reference [1] for a detailed bibliography): such systems were studied using Hill's determinant method [1], normal forms [9, 12] or multiple scales [1]. Stability analysis of elastic systems was investigated by Bolotin [19]. The stability limit of parametrically excited systems has been investigated via Fourier series [20] and recently via a generalized Bolotin method [21]. Stability analysis of periodic systems was also discussed by Guttalu *et al.* [22] using truncated point mappings and several results were presented for the Mathieu equation. In the successive papers [23, 24], Sinha *et al.* developed an original technique in order to investigate the stability of

non-linear systems. By combining Chebyshev polynomial expansions and Lyapunov–Floquet transform, a time-invariant form for periodic time-dependent systems was successfully obtained; a higher order analysis via normal form and symbolic computations was then considered. These methods seem to be very powerful, but mixed techniques still have to be coupled (Chebyshev expansions, normal form analysis, etc.).

Numerical methods have been developed, first to find periodic solutions and second, to follow such solutions by continuation techniques [25] or to study Poincaré mapping numerically. Searching periodic solutions using continuation techniques (or fixed point of a Poincaré map) often increases the dimension of ordinary differential equations that have to be solved using standard integration methods (of the Runge–Kutta type for example) and the Newton method [26]. Generally speaking, it is neither possible nor convenient to use the same numerical method to look upon periodic solutions of the original non-linear system and to study the behaviour of the linearized system (around this first periodic solution). Very often, only transitions between stable and unstable areas in the parameter space are sought for they correspond to periodic orbits.

Usually, the quantitative behaviour of periodic systems is studied using one of these analytical (perturbation, averaging, point mappings, etc.) or numerical (continuation, etc.) methods. Clearly, analytical methods have their own limitations essentially due to the question of small parameters; only parametric excitations of small amplitude may be determined accurately. As mentioned in reference [24], point mappings require an exact or an approximate solution of the original non-linear problem. Therefore, each method belonging to the family of "analytical methods" carries its own limitation. Purely numerical methods are also self-limited in the sense that very often, only transition curves can be provided when periodic solutions involved in the Floquet theory are considered, or they face severe drawbacks partly due to time-integration costs and the dimension of both phase space and parameter space.

In this paper, it is intended to introduce a new Galerkin procedure based on wavelet series expansions of signals and operators involved in the mathematical setting. Qualitatively, this method intends to provide a hybrid technique; a numerical method for the "skeleton" of the parametric system is numerically computed using wavelet representations of integral (resp. differential) operators, which is an analytical method because of the matrix representation of operators. This new method will be used both to compute periodic (stationary) and non-periodic solutions (transient) of time-varying systems so that stability analysis could be obtained including quantization of stability. The topic of the present paper is to restrict the scope of the wavelet-Galerkin procedure to the computation of transient responses of parametrically excited systems and to the stability analysis of linear systems. Extensions are nevertheless forthcoming such as for the search of periodic orbits of linear and also non-linear dynamical systems. Based on a wavelet analysis, the method inherits interesting properties of wavelets (localization, universal approximation of very general signals and operators) to furnish the framework of a genuine multi-resolution approach to study the dynamical response of parametrically excited systems, eventually including both non-smooth and monitored time-varying components.

The paper is organized as follows: in section 1, the class of parametrically excited systems considered in the present study is emphasized. Section 2 introduces the wavelet-Galerkin procedure used to seek the transient response (periodic or not) of general dynamical systems and numerical experiments are conducted including several single and multi-degree-of-freedom (d.o.f.) parametrically excited systems. In section 3, the wavelet tool is used to compute the transition matrix of the Floquet theory and to characterize stability/instability levels of a single and a two d.o.f. system. Finally, some conclusions and proposed future work are outlined.

2. A CLASS OF SECOND ORDER DIFFERENTIAL PROBLEMS WITH TIME-VARYING COEFFICIENTS

As there is interest in analyzing the stability problem or the dynamical response of a multi-d.o.f. system of N coupled oscillators, two classes of problems governed by second order systems of linear differential equations with time-varying coefficients are considered, depicted using matrix notations as

$$(P)\ \begin{vmatrix} \ddot{\mathbf{X}}(t) + \boldsymbol{A}(t)\dot{\mathbf{X}}(t) + \boldsymbol{F}(t)\mathbf{X}(t) = \mathbf{G}(t) & \begin{bmatrix}\text{Dynamical}\\ \text{Response}\end{bmatrix}, \\ \mathbf{X}(0) = \mathbf{X}_0, \quad \dot{\mathbf{X}}(0) = \dot{\mathbf{X}}_0 \end{vmatrix}$$

$$(P_s)\ |\ddot{\mathbf{X}}(t) + \boldsymbol{H}_1(t, \boldsymbol{\lambda})\dot{\mathbf{X}}(t) + \boldsymbol{H}_2(t, \boldsymbol{\lambda})\mathbf{X}(t) = \mathbf{0} \quad [\text{Stability}], \tag{1}$$

where $\mathbf{X}(t) = [X_i(t)]_{1 \leqslant i \leqslant N}$ is the system response, $\boldsymbol{A}(t), \boldsymbol{F}(t), \boldsymbol{H}_1(t, \boldsymbol{\lambda}), \boldsymbol{H}_2(t, \boldsymbol{\lambda})$ are matrices of T-periodic time-varying functions, standing, respectively, for gyroscopic terms (eventually including viscous damping effects) and parametric excitations, $\mathbf{G}(t)$ is an external forcing, $(\mathbf{X}_0, \dot{\mathbf{X}}_0)$ are the initial conditions and $\boldsymbol{\lambda}$ denotes a set of parameters.

3. THE WAVELET-GALERKIN PROCEDURE

The basic idea of the wavelet-Galerkin procedure consists in searching for solutions of parametric systems (1) as a wavelet series expansion of T-periodic wavelet patterns derived from a basis of Daubechies wavelet [27] using a Poisson periodization technique [28]. This approach requires the second order form of systems (1) to be explained in wavelet bases in order to transform the original system into a matrix problem involving wavelet representations of integral (resp. differential) operators, gyroscopic and parametric excitations, external forcing and of system response. As the theory of multi-resolution analysis developed by Mallat [29] is the accurate theoretical framework providing Hilbert bases of spaces $L^2(\mathbb{R})$ and $L^2(\mathbb{R}/T\mathbb{Z})$ [30] (standing for the space of T-periodic signals of finite energy), the next sections briefly recall the basic principles of a periodic multi-resolution analysis and define discrete representations of signals and operators in wavelet bases. Though functional background and notations are depicted hereafter, the reader is invited to refer to references [29, 31] for thorough explanations.

3.1. MULTI-RESOLUTION ANALYSIS OF $L^2(\mathbb{R}/T\mathbb{Z})$

A multi-resolution analysis (MRA) of a periodic signal X belonging to $L^2(\mathbb{R}/T\mathbb{Z})$ consists in building successive approximations $(X^j)_{0 \leqslant j \leqslant J}$ of X including details $(X^{d_i})_{0 \leqslant i \leqslant j}$ at a resolution 2^{-j}, the scale $j = 0$ and J standing, respectively, for the coarser and the finer scales. An MRA of $L^2(\mathbb{R}/T\mathbb{Z})$ is obtained by folding an MRA of $L^2(\mathbb{R})$ on itself using the Poisson summation technique.

As far as mathematics is concerned, an MRA of $L^2(\mathbb{R}/T\mathbb{Z})$ is defined as a sequence $(V_j)_{j \in \mathbb{N}}$ of nested subspaces of $L^2(\mathbb{R}/T\mathbb{Z})$ spanned by an orthonormal basis of 2^j scaling patterns $(\varphi_{jk})_{0 \leqslant k < 2^j}$ (see for instance, periodized Daubechies scaling functions of order 4 in Figure 1) obtained by combining periodization and dilation/shifting of a single father wavelet (namely the scaling function φ) via the relationship

$$\varphi_{jk}(t) = 2^{j/2} \sum_{r \in \mathbb{Z}} \varphi\left(2^j\left(\frac{t}{T} + r\right) - k\right). \tag{2}$$

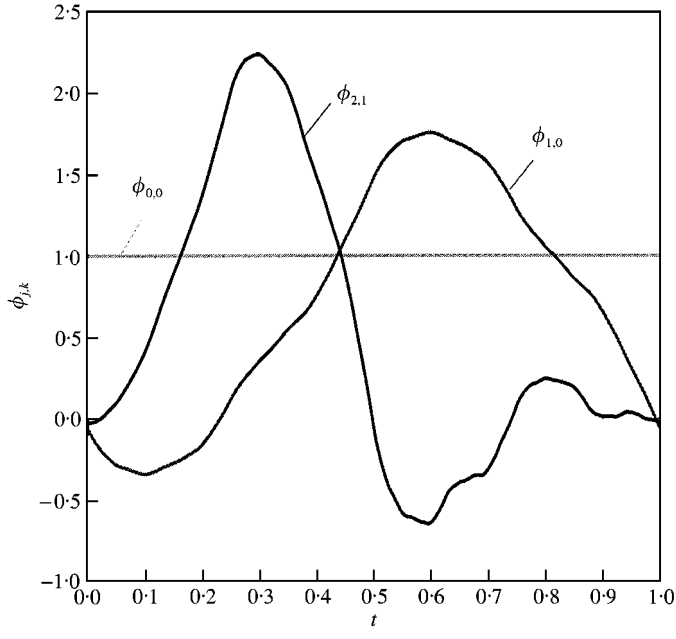

Figure 1. Periodized Daubechies scaling functions φ_{00}, φ_{10}, φ_{21} of order 4.

The approximation spaces V_j check the following properties:

$$\text{(Closure)} \quad \bigcap_j V_j = \{0\}, \qquad \overline{\bigcup_j V_j} = L^2(\mathbb{R}/T\mathbb{Z}), \tag{3}$$

$$\text{(Nested spaces)} \quad V_j \subseteq V_{j+1} \subseteq L^2(\mathbb{R}/T\mathbb{Z}), \tag{4}$$

$$\text{(Shifting)} \quad f \in V_j \Leftrightarrow f\left(\cdot - \frac{kT}{2^j}\right) \in V_j, \tag{5}$$

$$\text{(Dilation)} \quad f \in V_j \Leftrightarrow f(2\cdot) \in V_{j+1}, \tag{6}$$

$$\text{(Orthonormal basis)} \quad V_j = \text{Span}\{\varphi_{jk}\}_{0 \leqslant k < 2^j}, \tag{7}$$

$$\text{(Coarse space)} \quad V_0 = \text{Span}\{1\}. \tag{8}$$

In order to measure the difference between two successive approximations X^j and X^{j+1} of signal X, respectively, in V_j and V_{j+1}, detail spaces W_j are introduced as the orthogonal supplementary spaces of V_j in V_{j+1} depicted by

$$V_{j+1} = V_j \overset{\perp}{\oplus} W_j. \tag{9}$$

Similarly, spaces W_j are spanned by an orthonormal basis of dimension 2^j of wavelet patterns $(\psi_{jk})_{0 \leqslant k < 2^j}$ (see, for instance, periodized Daubechies wavelets of order 4 in Figure 2) obtained when combining periodization and dilation/shifting of a single mother

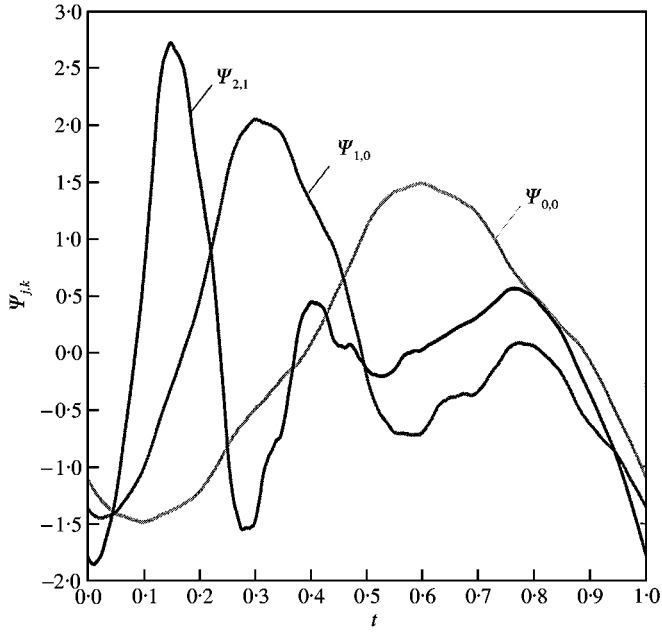

Figure 2. Periodized Daubechies wavelets $\psi_{00}, \psi_{10}, \psi_{21}$ of order 4.

wavelet ψ via the relationship

$$\psi_{jk}(t) = 2^{j/2} \sum_{r \in \mathbb{Z}} \psi\left(2^j\left(\frac{t}{T} + r\right) - k\right). \tag{10}$$

Hence, similar properties hold for spaces W_j

$$\text{(Superposition of details)} \quad L^2(\mathbb{R}/T\mathbb{Z}) = V_0 \overset{\perp}{\bigoplus_{j \in \mathbb{Z}}} W_j, \tag{11}$$

$$\text{(Refinement)} \quad V_j = V_0 \overset{\perp}{\bigoplus_{0 \leqslant i \leqslant j}} W_i, \tag{12}$$

$$\text{(Shifting)} \quad f \in W_j \Leftrightarrow f\left(\cdot - \frac{kT}{2^j}\right) \in W_j, \tag{13}$$

$$\text{(Dilation)} \quad f \in W_j \Leftrightarrow f(2\cdot) \in W_{j+1}, \tag{14}$$

$$\text{(Orthonormal basis)} \quad W_j = \text{Span}\,\{\psi_{jk}\}_{0 \leqslant k < 2^j}. \tag{15}$$

In practice, the construction of the mother wavelet ψ derives from the scaling function φ which also derives from the determination of admissible filtering functions [27, 31].

Associating the common inner product $\langle f, g \rangle = 1/T \int_0^T f(t)\,\overline{g(t)}\,\mathrm{d}t$ to $L^2(\mathbb{R}/T\mathbb{Z})$, a signal approximation X^J of X at resolution J may indifferently be approximated with the scaling

or with the wavelet series expansions:

$$X(t) \simeq X^J(t) = \mathbf{S}^J(X) \cdot \boldsymbol{\varphi}^J(t) \tag{16}$$

$$= \sum_{k=0}^{2^J-1} S^{Jk}(X)\varphi_{Jk}(t) \tag{17}$$

$$= \mathbf{S}^0(X) \cdot 1 + \sum_{j=0}^{J-1} \mathbf{D}^j(X) \cdot \boldsymbol{\psi}^j(t) \tag{18}$$

$$= S^{00}(X) + \sum_{j=0}^{J-1} \sum_{k=0}^{2^j-1} D^{jk}(X)\psi_{jk}(t), \tag{19}$$

where

- $\boldsymbol{\varphi}^J(t) = [\varphi_{Jk}(t)]_{0 \leqslant k < 2^J}^{\mathrm{T}}$ is the collection of scaling function patterns,
- $\boldsymbol{\psi}^j(t) = [\psi_{jk}(t)]_{0 \leqslant k < 2^j}^{\mathrm{T}}$ is the collection of wavelet patterns,
- $\mathbf{S}^J(X) = [(\mathbf{S}_1{}^{Jk}(X))_{0 \leqslant k < 2^J} \cdots (\mathbf{S}_N{}^{Jk}(X))_{0 \leqslant k < 2^J}]^{\mathrm{T}}$ is the arranged sequence of scaling coefficients of $X(t)$ at resolution J,
- $\mathbf{D}^j(X) = [(\mathbf{D}_1^{jk}(X))_{0 \leqslant k < 2^j} \cdots (\mathbf{D}_N^{jk}(X))_{0 \leqslant k < 2^j}]^{\mathrm{T}}$ is the arranged sequence of wavelet coefficients of $X(t)$ at scale j

involving the inner products $S^{jk}(X) = \langle X, \varphi_{jk} \rangle_{L^2(\mathbb{R}/T\mathbb{Z})}$ and $D^{jk}(X) = \langle X, \psi_{jk} \rangle_{L^2(\mathbb{R}/T\mathbb{Z})}$ which, respectively, refer to the scaling coefficients and the wavelet coefficients of signal X.

Practically speaking, time-scale analysis of a periodic signal may easily be performed using fast tree algorithms [29] permitting an easy extraction or cancellation of details channels in a (monitored) signal X living near resolution scales $j \in [0, J]$.

The down-scaling scheme (detailed in the periodical case [27, pp. 934–938; 28, pp. 55–59] and depicted in Figure 3) consists of successively convoluting scaling representation $\mathbf{S}^J(X)$ of a signal X with a low-pass filter H_j and a band-pass filter G_j and then down-sampling the coefficients obtained by a factor of two (convolution and down-sampling calculations being performed in the Fourier space). By the end, scaling coefficients $\mathbf{S}^j(X)$ and wavelet coefficients $\mathbf{D}^j(X)$ are recursively computed from the coefficients $\mathbf{S}^{j+1}(X)$ at scale $(j+1)$ with a complexity of order $O(N)$. Moreover, this transformation is reversible and the lifting scheme consists of similar convolutions and over-sampling operations. Finest scaling coefficients $\mathbf{S}^J(X)$ are computed using adaptive numerical integration procedures [32, 33] specifically developed in the framework of periodized compactly supported Daubechies wavelets.

3.2. TIME-SCALE REPRESENTATION OF SIGNAL RESPONSE

Considering an N d.o.f.s system, the time-scale representation of vector $\mathbf{X}(t)$ derives directly from the previous case and is expressed in the harmonic wavelet basis by

$$\mathbf{X}(t) \simeq \mathbf{X}^J(t) = \boldsymbol{\Phi}^J(t) \cdot \mathbf{S}^J(\mathbf{X}) \tag{20}$$

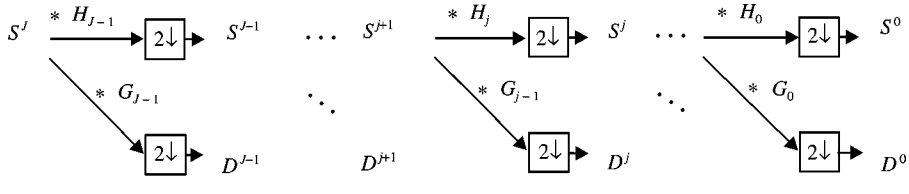

Figure 3. Pyramidal decomposition tree of a signal in periodic wavelets.

$$= \sum_{k=0}^{2^J-1} \mathbf{S}^{Jk}(\mathbf{X}) \cdot \varphi_{Jk}(t) \tag{21}$$

$$= \boldsymbol{\Phi}^0(t) \cdot \mathbf{S}^0(\mathbf{X}) + \sum_{j=0}^{J-1} \boldsymbol{\Psi}^j(t) \cdot \mathbf{D}^j(\mathbf{X}) \tag{22}$$

$$= \mathbf{S}^0(\mathbf{X}) + \sum_{j=0}^{J-1} \sum_{k=0}^{2^j-1} \mathbf{D}^{jk}(\mathbf{X}) \cdot \psi_{jk}(t), \tag{23}$$

where

- $\boldsymbol{\Phi}^J(t) = \boldsymbol{I}_N \otimes [\boldsymbol{\varphi}^J(t)]^{\mathrm{T}}$ is a tensor product of scaling function patterns,
- $\boldsymbol{\Psi}^J(t) = \boldsymbol{I}_N \otimes [\boldsymbol{\psi}^J(t)]^{\mathrm{T}}$ is a tensor product of wavelet patterns,
- $\mathbf{S}^J(\mathbf{X}) = [(\mathbf{S}_1{}^{Jk}(\mathbf{X}))_{0 \leqslant k < 2^J} \cdots (\mathbf{S}_N{}^{Jk}(\mathbf{X}))_{0 \leqslant k < 2^J}]^{\mathrm{T}}$ is the vertical concatenation of scaling coefficients sequences of $\mathbf{X}(t)$ at resolution J,
- $\mathbf{D}^j(\mathbf{X}) = [(\mathbf{D}_1{}^{jk}(\mathbf{X}))_{0 \leqslant k < 2^j} \cdots (\mathbf{D}_N{}^{jk}(\mathbf{X}))_{0 \leqslant k < 2^j}]^{\mathrm{T}}$ is the vertical concatenation of wavelet coefficients sequence at scale j.

3.3. TIME-SCALE REPRESENTATION OF OPERATORS

Consider an operator $\mathscr{T}$ belonging to either $\mathscr{L}(L^2(\mathbb{R}/T\mathbb{Z}), L^2(\mathbb{R}))$ or $\mathscr{L}(L^2(\mathbb{R}), L^2(\mathbb{R}))$ denoting the spaces of continuous linear mappings, respectively, from $L^2(\mathbb{R}/T\mathbb{Z})$ onto $L^2(\mathbb{R})$ and from $L^2(\mathbb{R})$ onto $L^2(\mathbb{R})$. As the intention is to expand operator $\mathscr{T}$ in the multi-resolution spaces $(V_j)_{j \in \mathbb{N}}$, the wavelet approximation operator $\mathscr{T}_J : V_J \to V_J$ of $\mathscr{T}$ is defined at the finer resolution J and depicted hereafter as

$$\begin{aligned} \mathscr{T} \Big| & \begin{array}{ll} L^2(\mathbb{R}/T\mathbb{Z}) \text{ or } L^2(\mathbb{R}) & \to L^2(\mathbb{R}), \\ u & \to v = \mathscr{T} u, \end{array} \\ \wr & \\ \mathscr{T}_J \Big| & \begin{array}{l} V_J \to V_J, \\ u_J \to v_J = \mathscr{T}_J u_J = (P_J \mathscr{T} P_J) u_J. \end{array} \end{aligned} \tag{24}$$

Introducing orthogonal projectors

$$P_j : L^2\left(\frac{\mathbb{R}}{T\mathbb{Z}}\right) \text{ or } L^2(\mathbb{R}) \to V_j, \tag{25}$$

$$Q_j : L^2\left(\frac{\mathbb{R}}{T\mathbb{Z}}\right) \text{ or } L^2(\mathbb{R}) \to W_j, \tag{26}$$

respectively, onto V_j and W_j, the non-standard form of operator $\mathscr{T} \simeq \mathscr{T}_J = P_J \mathscr{T} P_J$ is expressed as depicted by Beylkin [34, 35]. Recursively equating $\mathscr{T}_J = P_J \mathscr{T} P_J = (P_{J-1} + Q_{J-1}) \mathscr{T} (P_{J-1} + Q_{J-1})$, the formal telescopic series is

$$\mathscr{T} \simeq \mathscr{T}_J = \mathscr{T}_0 + \sum_{j=0}^{J-1} (\mathscr{G}_j + \mathscr{A}_j + \mathscr{B}_j) \tag{27}$$

and the following recursive definition of $\mathscr{T}$

$$\mathscr{T}_j = \begin{bmatrix} \mathscr{A}_{j-1} & \mathscr{B}_{j-1} \\ \mathscr{G}_{j-1} & \mathscr{T}_{j-1} \end{bmatrix}, \tag{28}$$

where

$$\mathscr{G}_j = P_j \mathscr{T} Q_j : W_j \to V_j, \tag{29}$$

$$\mathscr{A}_j = Q_j \mathscr{T} Q_j : W_j \to W_j, \tag{30}$$

$$\mathscr{B}_j = Q_j \mathscr{T} P_j : V_j \to W_j \tag{31}$$

are scale-to-scale operator contributions.

Hence, the operator $\mathscr{T}$ may be approximated using its non-standard representation

$$\mathscr{T} \simeq \mathscr{T}_J = \{\{\mathscr{G}_j, \mathscr{A}_j, \mathscr{B}_j\}_{0 \leqslant j \leqslant J-1}, \mathscr{T}_0\} \tag{32}$$

in the wavelet basis

$$\{\varphi(\cdot - k)\varphi(\cdot - l), \{\psi_{jk}\varphi_{jl}, \psi_{jk}\psi_{jl}, \varphi_{jk}\psi_{jl}\}_{j \geqslant 0}\}_{(k,l) \in \mathbb{Z}^2} \tag{33}$$

$$(\text{resp. } \{1, \{\psi_{jk}\varphi_{jl}, \psi_{jk}\psi_{jl}, \varphi_{jk}\psi_{jl}\}_{0 \leqslant k,l < 2^j}^{j \geqslant 0}\}) \tag{34}$$

of $L^2(\mathbb{R}^2)$ (resp. $L^2([\mathbb{R}/T\mathbb{Z}]^2)$). This operator representation, depicted in reference [35] which nearly uncouples all scaling interactions, is characterized by an optimally minimized band structure. Contrary to the standard form, the non-standard form permits an efficient reduction of operators to a sparse narrowbanded form with the availability of $O(N)$ inverse matrix algorithms. It also exhibits a built-in pre-conditioner featuring power of two multipliers ensuring accurate inversions of matrix systems. Hence, using a well-localized wavelet analysis has multiple advantages against an "analytical" Fourier analysis which results in full and badly conditioned matrix systems. The reader may refer to reference [35] for further details.

Time-scale representation $\mathbf{S}^J(v_J)$ of signal approximation $v_J = \mathscr{T}_J u_J$ may be computed from $\mathbf{S}^J(u_J)$ of signal approximation u_J using matrix representation $\boldsymbol{T}^J(\mathscr{T})$ of $\mathscr{T}_J$ when equating

$$\mathbf{S}^J(v_J) = \boldsymbol{T}^J \cdot \mathbf{S}^J(u_J), \tag{35}$$

which involves the inner products

$$\boldsymbol{T}^J = \langle \mathscr{T}(\varphi_{Jl}), \varphi_{Jk} \rangle_{0 \leqslant k,l < 2^J}. \tag{36}$$

Similar expressions also hold for scale-to-scale components $\mathscr{G}_j$, $\mathscr{A}_j$, $\mathscr{B}_j$ as depicted in equations (37)–(39) and are

$$\boldsymbol{\Gamma}^j = \langle \mathscr{T}(\psi_{jl}), \varphi_{jk} \rangle_{0 \leqslant k,l < 2^j}, \tag{37}$$

$$\boldsymbol{A}^j = \langle \mathscr{T}(\psi_{jl}), \psi_{jk} \rangle_{0 \leqslant k,l < 2^j}, \tag{38}$$

$$\boldsymbol{B}^j = \langle \mathscr{T}(\varphi_{jl}), \psi_{jk} \rangle_{0 \leqslant k,l < 2^j}. \tag{39}$$

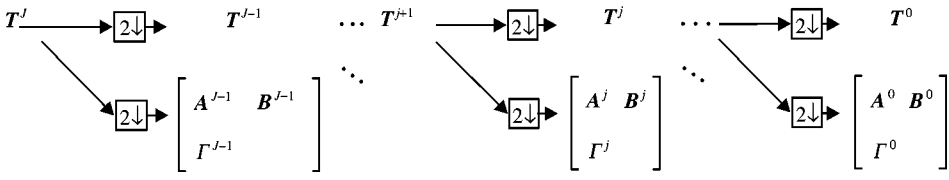

Figure 4. Pyramidal decomposition tree of an operator in periodic wavelets.

As in section 3.1, fast tree algorithms illustrated in Figure 4 are also available to successively compute time-scale representation $\boldsymbol{T}^j$ of $\mathscr{T}_j$ from the finer matrix approximation $\boldsymbol{T}^J$ of $\mathscr{T}_J$ with a complexity of order $O(N)$. Matrix representation $\boldsymbol{T}^j$ is successively convoluted with a low-pass/low-pass filter $\mathbf{H}_j \otimes \mathbf{H}_j$ to obtain matrix $\boldsymbol{T}^{j-1}$ of $\mathscr{T}_{j-1}$ at scale $j-1$, with a band-pass/low-pass filter $\mathbf{H}_j \otimes \mathbf{G}_j$ to obtain matrix $\boldsymbol{\Gamma}^{j-1}$ of $\mathscr{G}_{j-1}$, with a band-pass/band-pass filter $\mathbf{G}_j \otimes \mathbf{G}_j$ to obtain matrix $\boldsymbol{A}^{j-1}$ of $\mathscr{A}_{j-1}$, with a low-pass/band-pass filter $\mathbf{G}_j \otimes \mathbf{H}_j$ to obtain matrix $\boldsymbol{B}^{j-1}$ of $\mathscr{B}_{j-1}$ and then downsampled by a factor of two. The lifting scheme, which consist of reconstructing the finer approximation $\boldsymbol{T}^J$ from the collection $\{(\boldsymbol{\Gamma}^j, \boldsymbol{A}^j, \boldsymbol{B}^j\}_{0 \leqslant j < J}, \boldsymbol{T}^0\}$, is based on the same principles. Adaptive numerical integration schemes were designed to compute the matrix representation of a few basic operators efficiently at the finest scale J.
Several features that are thoroughly developed in reference [36] consist of

- building wavelet-oriented quadrature formulae to compute efficiently truncated integrals of the type $\int_a^b f(t)\varphi(t)\,\mathrm{d}t$ where (a, b) are dyadic rationals ranging within the support of scaling function φ, f being any (sufficiently regular) signal to be analyzed,
- linking inner products featuring periodized scaling functions (in $L^2(\mathbb{R}/T\mathbb{Z})$) to inner products involving scaling functions of $L^2(\mathbb{R})$,
- using fast tree algorithms to compute inner products featuring dilated/shifted scaling patterns,
- computing the wavelet approximation $\boldsymbol{T}^J = \langle \mathscr{T}(\varphi_{Jl}), \varphi_{Jk} \rangle_{0 \leqslant k,l < 2^J}$.

The next section briefly describes the structure of the wavelet representation of two generic operators involved in the wavelet-Galerkin procedure, namely the product operator $\mathscr{T}_f$ and the integral operator $\mathscr{T}_\int$ given by

$$\mathscr{T}_f : U \to V \;/\; V(t) = f(t)U(t), \tag{40}$$

$$\mathscr{T}_\int : U \to V \;/\; V(t) = \int_0^t U(\tau)\,\mathrm{d}\tau. \tag{41}$$

3.3.1. *Time-scale representation of the product operator*

Given a smooth T-periodic signal $f \in L^2(\mathbb{R}/T\mathbb{Z})$, the self-adjoint operator $\mathscr{T}_f$ is defined by

$$\mathscr{T}_f \begin{vmatrix} L^2(\frac{\mathbb{R}}{T\mathbb{Z}}) \to L^2(\frac{\mathbb{R}}{T\mathbb{Z}}), \\ u \qquad\quad \to v = \mathscr{T} u = fu. \end{vmatrix} \tag{42}$$

Therefore, its wavelet counterpart $\mathscr{T}_f^J$ at scale J requires the computation of

$$\boldsymbol{T}_f^J(k,l) = \frac{1}{T}\int_0^T f(\tau)\varphi_{Jk}(\tau)\varphi_{Jl}(\tau)\,\mathrm{d}\tau \tag{43}$$

$$= \int_{N_{inf}}^{N_{sup}} f\left(\frac{T}{2^J}(x+k-N_{inf})\right)\varphi(x-(l-k))\varphi(x)\,\mathrm{d}x \quad 0 \leqslant k \leqslant l < 2^J, \tag{44}$$

where $[N_{inf}, N_{sup}]$ is the support of the scaling function φ.

Equation (44) is obtained by assuming that the criterion

$$\forall t \in [0, T] \quad \varphi_{J0}(t) = 2^{J/2}\varphi\left(2^J\frac{t}{T} + N_{inf}\right) \tag{45}$$

is valid for compactly supported Daubechies wavelets of order N [27] which only hold when scales $J \geqslant J_i = \max_{j\in\mathbb{N}}\{j/2^j \geqslant N_{sup} - N_{inf}\}$ are checked. The matrix representation of $\boldsymbol{T}_f^J$ has a sparse symmetric band structure as displayed in Figure 5 and whose bandwidth is related to the support of the analyzing wavelet. As product operators are required to model gyroscopic or parametric components in problems (1), derived following the linearization of a smooth non-linear dynamical system in the neighbourhood of a periodic solution, the wavelet representation was straightforwardly extended to cope with monitored multiplicative signals f approximated by wavelet series expansions at resolution J.

3.3.2. *Time-scale representation of the integral operator*

As the wavelet-Galerkin procedure requires integral forms of signals to be computed, the first integral operator $\mathscr{T}_\int$ is defined as

$$\mathscr{T}_f \begin{vmatrix} L^2(\frac{\mathbb{R}}{T\mathbb{Z}}) \to L^2([0,T]), \\ u \qquad\quad \to v = \mathscr{T}u/v(t) = \frac{1}{T}\int_0^t u(\tau)\,\mathrm{d}\tau\,. \end{vmatrix} \tag{46}$$

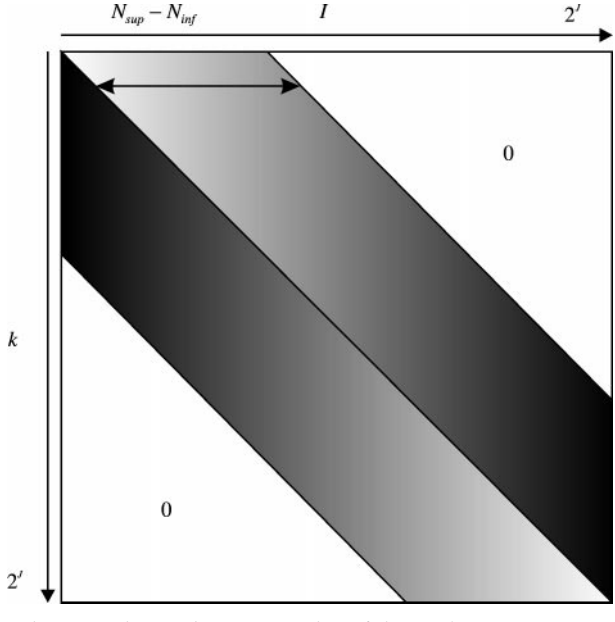

Figure 5. Time-scale representation of the product operator $\mathscr{T}_f$.

It is obvious that the periodicity of the image signal v is lost when applying $\mathscr{T}_{\int}$ to signal u. Despite a small Gibbs phenomenon eventually occurring near the edges, the harmonic wavelet representation is assumed to capture accurately the main features of operator $\mathscr{T}_{\int}$ within the frame window $[0, T]$. Yet this problem will soon vanish when considering relatively large resolution scales J.

Introducing $\Theta^J(t) = 1/T \int_0^t \varphi_{J0}(\tau)\,\mathrm{d}\tau$ as the first integrals of dilated scaling functions φ_{J0}, few properties hold for Θ^J and from equations (47) and (48)

$$\Theta^J(t) = 2^{-J/2} \begin{cases} \Theta(2^J \frac{t}{T} + N_{inf}) & \text{if } 0 \leqslant \frac{t}{T} < 2^{-J}(N_{sup} - N_{inf}), \\ \Theta(N_{sup}) & \text{if } 2^{-J}(N_{sup} - N_{inf}) \leqslant \frac{t}{T} < 1 \end{cases} \tag{47}$$

and

$$\forall t \in [0, T] \quad \begin{cases} \Theta^J(t - T) = \Theta^J(t) - \Theta^J(2^{-J} T(N_{sup} - N_{inf})), \\ \Theta^J(t + T) = \Theta^J(t) + \Theta^J(2^{-J} T(N_{sup} - N_{inf})), \end{cases} \tag{48}$$

where $\Theta(x) = \int_{N_{inf}}^{x} \varphi(u)\,\mathrm{d}u$ is given by expressions detailed in reference [37].
Matrix representation $\boldsymbol{T}_{\int}^J$ of approximation $\mathscr{T}_{\int}^J$ at scale J

$$\boldsymbol{T}_{\int}^J(k, l) = \frac{1}{T^2} \int_0^T \left(\int_0^t \varphi_{Jl}(\tau)\,\mathrm{d}\tau \right) \varphi_{Jk}(t)\,\mathrm{d}t \tag{49}$$

is then expressed in terms of $\Theta^J(t)$ when assuming $J \geqslant J_i$ and finally reduces to equations

$$2^J \boldsymbol{T}_{\int}^J(k, l) = \Theta(2^J - k + N_{inf}) + \Theta(N_{sup} + k - 1) - \Theta(2^J - 1 + N_{inf})$$

$$- \int_{N_{inf}}^{N_{sup} + k - 1} \Theta(x + l - k)\varphi(x)\,\mathrm{d}x \quad \text{if } 0 \leqslant 1 - k \leqslant (N_{sup} - N_{inf}) \tag{50}$$

$$= 0 \quad \text{if } (N_{sup} - N_{inf}) \leqslant 1 - k \text{ and } 1 \leqslant 2^J - (N_{sup} - N_{inf}) \tag{51}$$

$$= \Theta(2^J - k + N_{inf}) - \Theta(2^J - 1 + N_{inf}) \quad \text{if } (N_{sup} - N_{inf}) \leqslant 1 - k \leqslant 2^J$$

$$- (N_{sup} - N_{inf}) \text{ and } 1 \leqslant 2^J - (N_{sup} - N_{inf}) \tag{52}$$

$$= \Theta(2^J - k + N_{inf}) - \Theta(2^J - 1 + N_{inf}) - \int_{2^J + k - 1 + N_{inf}}^{N_{sup}}$$

$$\times \Theta(x + 1 - k - 2^J)\varphi(x)\,\mathrm{d}x \quad \text{if } 2^J - (N_{sup} - N_{inf}) < 1 - k \tag{53}$$

$$= \Theta(2^J - k + N_{inf}) - \int_{N_{inf} + k - 1}^{N_{sup}} \Theta(x + 1 - k)\varphi(x)\,\mathrm{d}x$$

$$\text{if } 0 < k - 1 < (N_{sup} - N_{inf}) \text{ and } 1 \leqslant 2^J - (N_{sup} - N_{inf}) \tag{54}$$

$$= \Theta(2^J - k + N_{inf}) - \Theta(2^J - 1 + N_{inf}) + \Theta(N_{sup})$$

$$- \int_{N_{inf} + k - 1}^{N_{sup}} \Theta(x + l - k)\varphi(x)\,\mathrm{d}x$$

$$\text{if } 0 < k-1 < (N_{sup} - N_{inf}) \text{ and } 1 > 2^J - (N_{sup} - N_{inf}) \tag{55}$$

$$= 1 \quad \text{if } k-1 \geqslant (N_{sup} - N_{inf}) \text{ and } k \leqslant 2^J - (N_{sup} - N_{inf}) \tag{56}$$

$$= \Theta(2^J - k + N_{inf}) \quad \text{if } (N_{sup} - N_{inf}) \leqslant k-1 < 2^J - (N_{sup} - N_{inf})$$

$$\text{and} \quad k > 2^J - (N_{sup} - N_{inf}) \tag{57}$$

$$= \Theta(2^J - k + N_{inf}) + \Theta(N_{sup} - 2^J + k - 1)$$

$$- \int_{N_{inf}}^{N_{sup} - 2^J + k - 1} \Theta(x + 2^J + l - k)\varphi(x)\,\mathrm{d}x$$

$$\text{if } k-1 \geqslant 2^J - (N_{sup} - N_{inf}). \tag{58}$$

Summing up, the matrix representation of $\mathscr{T}_{\int}^J$ highlights a sparse structure whose storage is similar to an arrow matrix as displayed in Figure 6. Two constant areas of values, respectively, 2^{-J} and 0 may be seen in Figure 6. Two non-trivial triangular areas also appear in the lower and upper corners because of the periodic analysis.

3.3.3. *Time-scale representation of matrix of operators*

Considering an N by N matrix $\mathscr{T}$ of operators $(\mathscr{T}_{ij})_{1 \leqslant i,j \leqslant N}$, its time-scale representation $\boldsymbol{T}^J$ derives directly from the previous section using a tensor product and is expressed in the harmonic wavelet basis of $V_J \otimes \cdots \otimes V_J$ by

$$\boldsymbol{T}^J = [\mathbb{1}_{(N,N)} \bigotimes \boldsymbol{T}_{ij}{}^J]_{1 \leqslant i,j \leqslant N}, \tag{59}$$

where $\mathbb{1}_{(N,N)}$ is the $N \times N$ unit matrix.

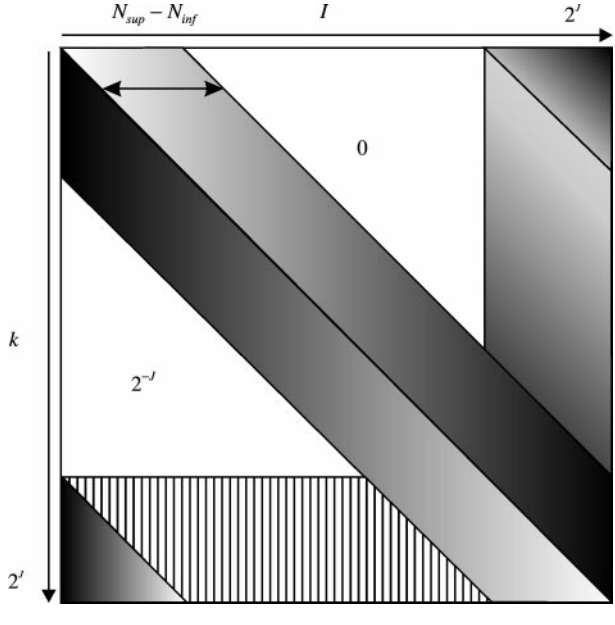

Figure 6. Time-scale representation of the integral operator $\mathscr{T}_{\int}$.

3.4. THE WAVELET-GALERKIN PROBLEM

Integrating system (P) between 0 and t, yields the $2N$ d.o.f. integral problem $P(Y)$ involving the time response and its derivative $\mathbf{Y} = [\mathbf{X}\ \dot{\mathbf{X}}]^{\mathrm{T}} = [\mathbf{Y}_1\ \mathbf{Y}_2]^{\mathrm{T}}$ solution of the first integral problem

$$P(Y)\ \left|\begin{array}{l} \mathbf{Y}_1(t) - \displaystyle\int_0^t \mathbf{Y}_2(\tau)\,\mathrm{d}\tau = \mathbf{X}_0 \\ \mathbf{Y}_2(t) + \displaystyle\int_0^t \boldsymbol{A}(\tau)\cdot\mathbf{Y}_2(\tau)\,\mathrm{d}\tau + \int_0^t \boldsymbol{F}(\tau)\cdot\mathbf{Y}_1(\tau)\,\mathrm{d}\tau = \dot{\mathbf{X}}_0 + \displaystyle\int_0^t \mathbf{G}(\tau)\,\mathrm{d}\tau. \end{array}\right. \tag{60}$$

Next, defining operators

$$\begin{aligned} \mathscr{T}_{\int} &: \mathbf{U} \to \mathbf{V} \ /\ \mathbf{V}(t) = \int_0^t \mathbf{U}(\tau)\,\mathrm{d}\tau, \\ \mathscr{T}_{\int}\mathscr{T}_A &: \mathbf{U} \to \mathbf{V} \ /\ \mathbf{V}(t) = \int_0^t \boldsymbol{A}(\tau)\cdot\mathbf{U}(\tau)\,\mathrm{d}\tau, \\ \mathscr{T}_{\int}\mathscr{T}_F &: \mathbf{U} \to \mathbf{V} \ /\ \mathbf{V}(t) = \int_0^t \boldsymbol{F}(\tau)\cdot\mathbf{U}(\tau)\,\mathrm{d}\tau, \end{aligned} \tag{61}$$

where $\mathscr{T}_{\int} = \boldsymbol{I}_{(N,N)} \otimes \mathscr{T}_{\int}$, $\mathscr{T}_A = [\mathbb{1}_{(N,N)} \otimes \mathscr{T}_{A_{ij}}]_{1 \leqslant i,j \leqslant N}$ and $\mathscr{T}_F = [\mathbb{1}_{(N,N)} \otimes \mathscr{T}_{F_{ij}}]_{1 \leqslant i,j \leqslant N}$ are, respectively, a vector of the integral operator and matrices of product operators, the wavelet-Galerkin problem is built using time-scale representations of $\mathscr{T}_{\int}$, $\mathscr{T}_{\int}\mathscr{T}_A$ and $\mathscr{T}_{\int}\mathscr{T}_F$ at the finer resolution scale J. Transient responses of system $P(Y)$ are derived directly using a wavelet condensation of equation (60) and their related scaling representation $\mathbf{S}^J(\mathbf{Y})$ may be found when solving the equivalent matrix problem

$$P^J(Y)\ \left|\begin{array}{l} \mathbf{S}^J(\mathbf{Y}_1) - [\boldsymbol{I}_{(N,N)} \bigotimes \boldsymbol{T}_{\int}^J]\cdot\mathbf{S}^J(\mathbf{Y}_2) = \mathbf{S}^J(\mathbf{X}_0), \\ \mathbf{S}^J(\mathbf{Y}_2) + [\mathbb{1}_{(N,N)} \bigotimes (\boldsymbol{T}_{\int}^J\ \boldsymbol{T}_{A_{ij}}^J)]_{ij}\cdot\mathbf{S}^J(\mathbf{Y}_2) \\ \qquad + [\mathbb{1}_{(N,N)} \bigotimes (\boldsymbol{T}_{\int}^J\ \boldsymbol{T}_{F_{ij}}^J)]\cdot\mathbf{S}^J(\mathbf{Y}_1) = [\boldsymbol{I}_{(N,N)} \otimes \boldsymbol{T}_{\int}^J]\cdot\mathbf{S}^J(\mathbf{G}) + \mathbf{S}^J(\dot{\mathbf{X}}_0). \end{array}\right. \tag{62}$$

Time-scale representations $\mathbf{S}^J(\mathbf{X}_0)$ and $\mathbf{S}^J(\dot{\mathbf{X}}_0)$ bound to initial conditions $(\mathbf{X}_0, \dot{\mathbf{X}}_0)$ are computed using a property of periodic wavelet analysis: space V_0 is spanned by constant functions. Consequently, the wavelet series $\mathbf{S}^0(\mathbf{X}_0)$ and $\mathbf{S}^0(\dot{\mathbf{X}}_0)$ at scale $J = 0$ are equal to the initial conditions $(\mathbf{X}_0, \dot{\mathbf{X}}_0)$ considering scaling approximations in V_0. Time-scale representations at scale J straight forwardly derive from the case $J = 0$ using the wavelet lifting scheme depicted in section 3.1. Interesting features related to the inner structure of problem $P^J(Y)$ may be pointed out: it is sufficient to pre-compute (once and for all) a few elementary block operators whose non-standard form in wavelet bases is sparse. Then, time responses may be obtained by solving the $(N2^J, N2^J)$ equivalent matrix system, which only requires a gathering of block operators, using a standard LU solver or a fast LU solver of order $O(N)$ available for wavelet non-standard forms as depicted in reference [38] and eventually taking into account a wavelet optimized pre-conditioner. This wavelet-Galerkin procedure permits multi-initial conditions inputs to proceed at the same time using a single LU decomposition. Indeed, the wavelet-Galerkin problem bound to any (non-smooth) gyroscopic (resp. parametric) components $\boldsymbol{A}(t)$ (resp. $\boldsymbol{F}(t)$) may easily be built thanks to

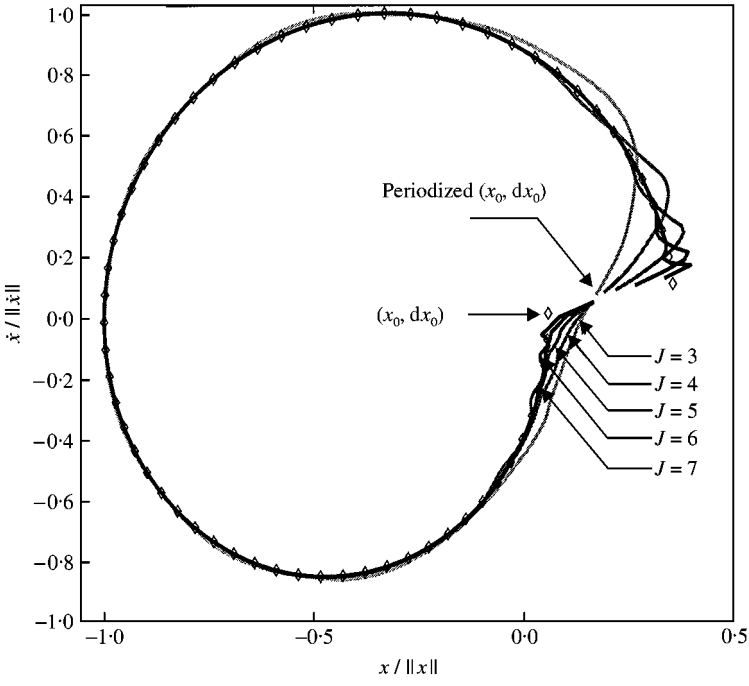

Figure 7. Simulation no. 1: phase portrait $[x/\|x\|, \dot{x}/\|\dot{x}\|]$; ◇◇◇◇, RK 45; ——, wavelets.

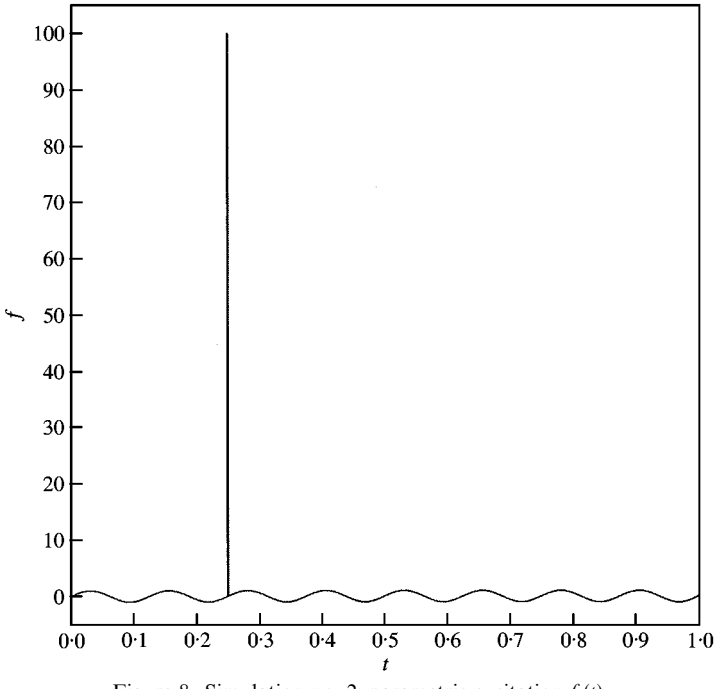

Figure 8. Simulation no. 2: parametric excitation $f_e(t)$.

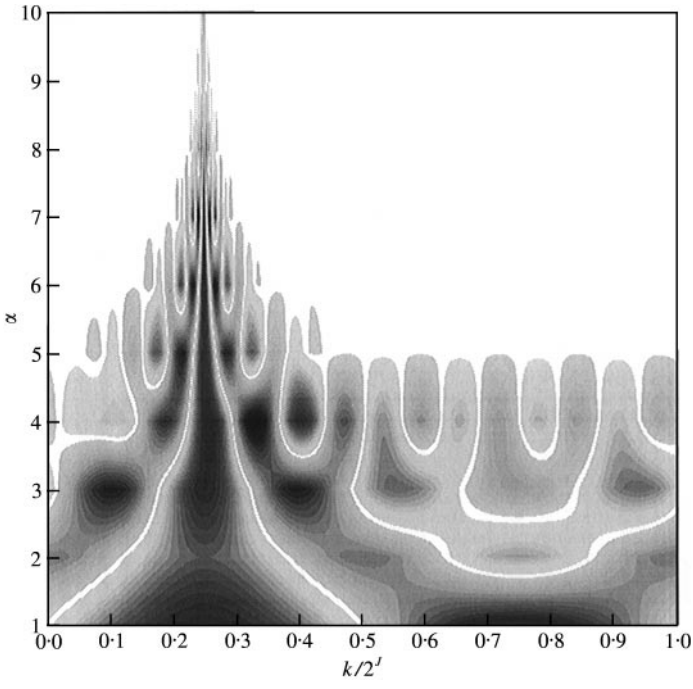

Figure 9. Simulation no. 2: wavelet pyramidal decomposition of $f_\varepsilon(t)$ in terms of $k/2^J$ and scales $\alpha = \log_2(2^J/m)$, $m \in [1, 2^{J-1}]$.

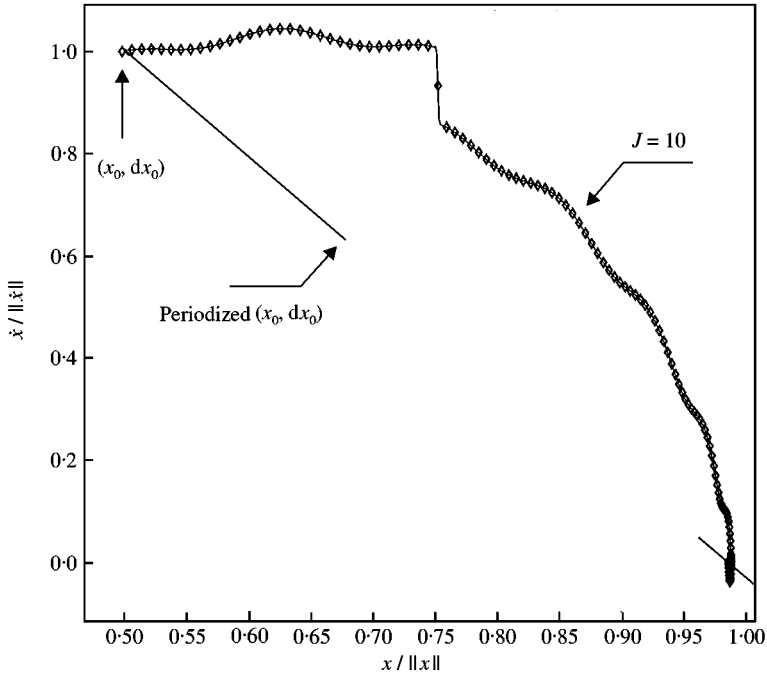

Figure 10. Simulation no. 2: phase portrait $[x/\|x\|, \dot{x}/\|\dot{x}\|]$; ◇◇◇◇, RK 45; ——, wavelets.

efficient computations of non-standard form of product operators involving monitored signals. Summing up, these features demonstrate that the wavelet procedure is both a numerical and an analytical method allowing the vibration of dynamical systems to be investigated.

In the following section, a few samples including one d.o.f. or multi-d.o.f. systems are investigated to demonstrate the reliability of the proposed wavelet-Galerkin procedure.

3.5. STUDY OF A CLASS OF SINGLE-(s.d.o.f.) SYSTEMS

The wavelet-Galerkin method is applied to search the transient response $(x, \dot{x})$ of one d.o.f. parametrically excited systems involving a damping factor a and whose dynamics are governed by

$$P_1 \begin{vmatrix} \ddot{x}(t) + a\dot{x} + f(t)x(t) = g(t), \\ x(0) = x_0, \quad \dot{x}(0) = \dot{x}_0, \quad f(t) = \omega_0^2 + \varepsilon f_\varepsilon(t), \\ a = \frac{10^{-1}}{2\pi}, \quad \omega_0 = 1 \text{ rad/s}, \quad \varepsilon = 1. \end{vmatrix} \tag{63}$$

Numerical simulations introduced according to several sets of parametric excitations $f(t)$, initial conditions and approximation scales J and gathered in Table 1 aim to emphasize the behaviour of the wavelet-Galerkin procedure on theoretical examples. Phase portraits of the dynamic responses are compared with those computed using a standard Runge–Kutta *RK*45 of order 4–5 integration scheme.

Simulation No. 1 involving a cosine parametric excitation aims to show that the wavelet method rapidly converges when increasing the resolution scale J by comparison with the reference solution computed with the Runge–Kutta scheme. The phase portrait displayed in Figure 7 in normalized co-ordinates $[x/\|x\|, \dot{x}/\|\dot{x}\|]$ according to several resolution scales J ranging between 3 (scaling series with eight patterns) and 7 (scaling series with 128 patterns) confirms the rapid convergence of solutions $(x^J, \dot{x}^J)$ even for coarse scales. However, a few side effects (large oscillations) near the time-window edges may be seen and are due to the periodization of non-periodic signals. That is why it is more convenient to speak of periodized initial conditions $(x_0, \dot{x}_0)$ rather than actual initial conditions. Moreover, these imperfections are reduced to a jump at the extremities of time interval (in order to get an artificial periodic signal from a non-periodic signal) when the approximation scale J becomes finer. In simulation no. 2, the sine parametric excitation is perturbed by a non-smooth (high frequency) accident as displayed in Figure 8. The wavelet pyramidal

TABLE 1

Numerical simulations

Excitation $f(t)$	Figures	J	$f_\varepsilon(t)$	$g(t)$	x_0	$\dot{x}_0$
Sinusoid	7	3–8	$\cos(2\pi t)$	$\varepsilon\cos^2(2\pi t) - 2a\pi\sin(2\pi t)$ $+ [\omega_0^2 - 4\pi^2]\cos(2\pi t)$	0·1	0·1
Perturbed sinusoid	8–10	10	100 if $\lvert t - \frac{1}{4}\rvert \leqslant 2^{-10}$ $\sin(16\pi\ t)$ if not	$\cos(2\pi t)$	0·5	1·0
Transition	11–13	7	$\cos(8\pi t)$ if $t < \frac{1}{2}$ $\cos(36\,\pi t)$ if $t > \frac{1}{2}$	$\cos(2\pi t)$	1·0	0·0
Noisy sinusoid	14–16	7	$x(t) = \boldsymbol{\varphi}^J(t)\cdot\mathbf{S}^J(x)$	$\cos(2\pi t)$	1·0	0·0

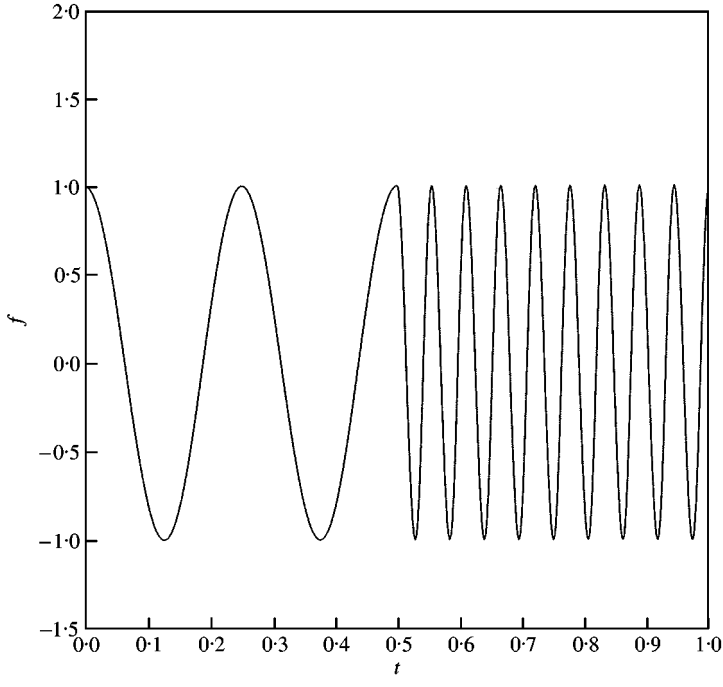

Figure 11. Simulation no. 3: parametric excitation $f_\varepsilon(t)$

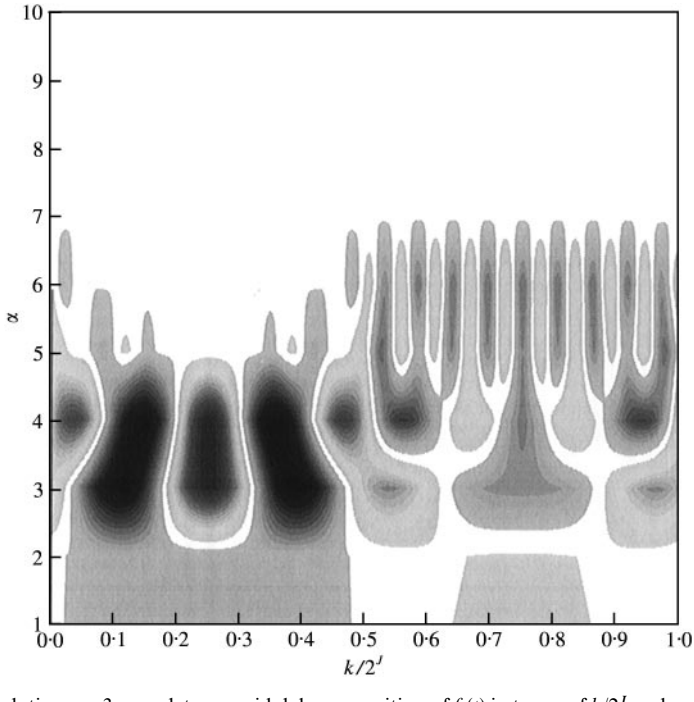

Figure 12. Simulation no. 3: wavelet pyramidal decomposition of $f_\varepsilon(t)$ in terms of $k/2^J$ and scales $\alpha = \log_2(2^J/m)$, $m \in [1, 2^{J-1}]$.

decomposition of $f_\omega(t)$ in Figure 9 demonstrates that the accident occurring near $t = \frac{1}{4}$ is very irregular with detailed components living up to the high-resolution scales. The phase portrait depicted in Figure 10 shows that results obtained with the wavelet method

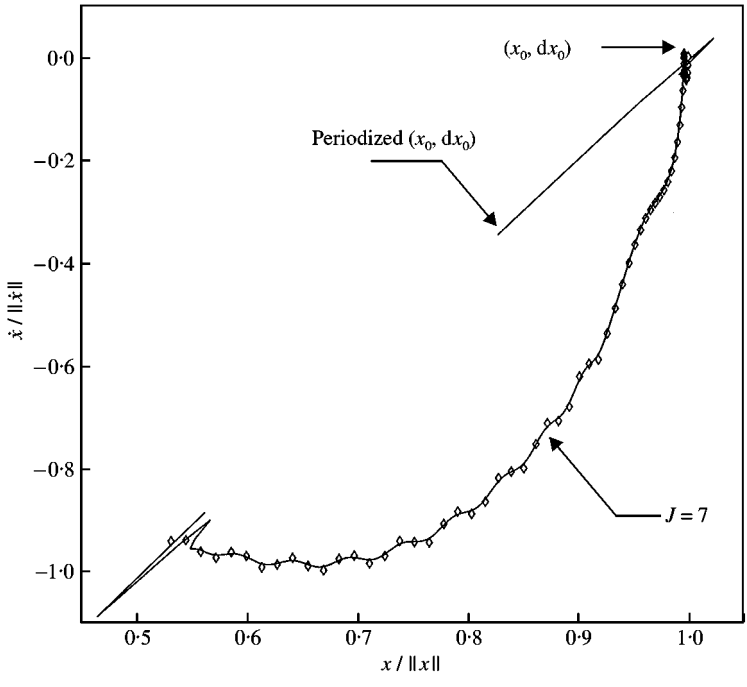

Figure 13. Simulation no. 3: diagram $[x/\|x\|, \dot{x}/\|\dot{x}\|]$; ◇ ◇ ◇ ◇, RK 45; ——, wavelets.

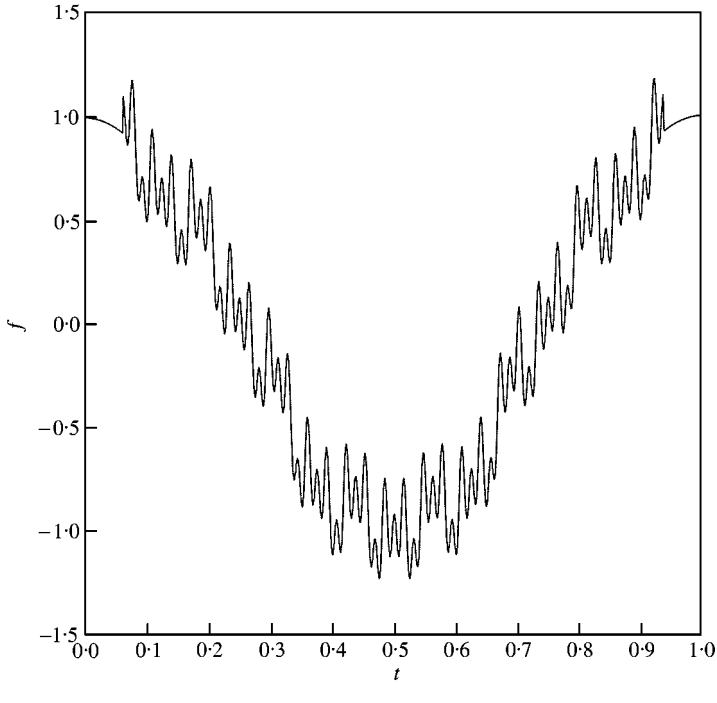

Figure 14. Simulation no. 4: parametric excitation $f_\varepsilon(t)$

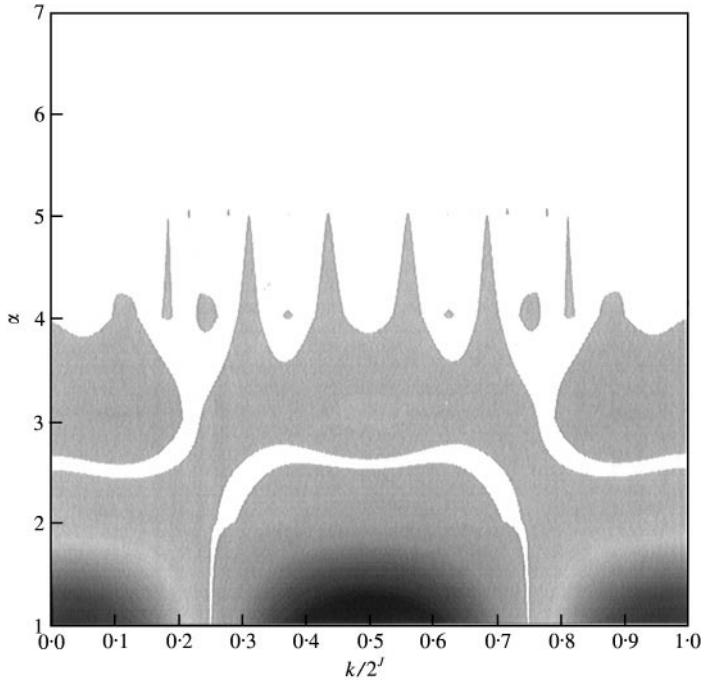

Figure 15. Simulation no. 4: wavelet pyramidal decomposition of $f_\varepsilon(t)$ in terms of $k/2^J$ and scales $\alpha = \log_2(2^J/m)$, $m \in [1, 2^{J-1}]$.

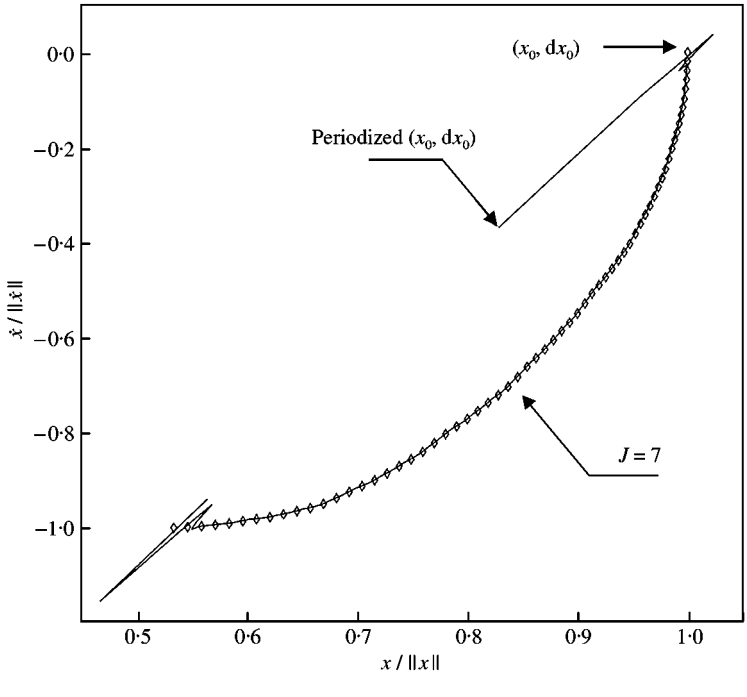

Figure 16. Simulation no. 4: diagram $[x/\|x\|, \dot{x}/\|\dot{x}\|]$; ◇◇◇◇, RK 45; ——, wavelets.

are in good agreement with the reference solution computed with a Runge–Kutta procedure.

In simulation no. 3, the parametric excitation is taken as a transition between a low and a high frequency cosine excitations (in Figure 11). The two characteristic frequencies may be distinguished in Figure 12 by looking for areas in which dominant wavelet coefficients are concentrated, the first one being near scale $J = 4$ before the transition takes place and the second higher frequency being near scale $J = 6$ after the transition. The sudden change in driving frequency may clearly be identified on the phase portrait depicted in Figure 13 with high frequency oscillations appearing after the transition.

Simulation No. 4 dealing with a noisy cosine parametric excitation (see Figures 14–16) shows that the wavelet method can accurately process irregular parametrically excited systems characterized by a continuous-band spectrum.

3.6. STUDY OF A MULTI-(m.d.o.f.) SYSTEM

In order to demonstrate that the wavelet procedure accurately encounters problems involving a relatively large number of d.o.f., the study now focuses on the following 10 d.o.f. parametrically excited system defined by

$$P_{10}\left|\begin{array}{l}\ddot{\mathbf{X}} + [a_i\delta_{ij}]_{i,j}\dot{\mathbf{X}} + [\omega_i\omega_j + \varepsilon_j\cos(\Omega_j t)]_{i,j}\mathbf{X} = \mathbf{G}(t),\\ \mathbf{X}(0) = [1]^{\mathrm{T}}_{1\leqslant i\leqslant N}, \quad \dot{\mathbf{X}}(0) = [a_i^2 - \Omega_i^2]^{\mathrm{T}}_{1\leqslant i\leqslant N},\\ a_i = \frac{10^{-1}}{2\pi}, \quad \omega_i = \sqrt{2^{1-i}}, \quad \Omega_i = 2\pi i, \quad \varepsilon_i = 2^{-i},\\ G_i(t) = \mathrm{e}^{a_i t}\left[a_i\Omega_i\sin(\Omega_i t)\right.\\ \qquad + \sum_{j=1}^{N}(\omega_i\omega_j - \Omega_i^2\delta_{ij})\cos(\Omega_j t)\\ \qquad \left. + \sum_{j=1}^{N}\varepsilon_j\cos^2(\Omega_j t)\right]\end{array}\right. \tag{64}$$

with known exponentially damped cosine responses

$$X_i(t) = \exp(a_i t)\cos(\Omega_i t) \quad \forall i \in [1, N]. \tag{65}$$

Figures 17 and 18 display the time responses and the derivatives of some components. Their corresponding phase portraits are illustrated in Figures 19 and 20. Despite a non-periodic problem being solved using a periodic wavelet analysis, the solutions still remain captured within the time window considered by comparison with a Runge–Kutta integration procedure. Only a few oscillations may be distinguished near the edges because the periodic analysis bends the solutions to lock them on a periodic cycle.

3.7. CONCLUDING REMARKS

Numerical experiments highlight reliable behaviour of the wavelet-Galerkin procedure to investigate the vibrations of parametrically excited systems and more generally systems with periodic time-varying coefficients. Though a light Gibbs phenomenon occurs near the edges, experiments demonstrate a rapid convergence of the approximations towards the reference Runge–Kutta solution, the accuracy being similar to a Runge–Kutta scheme.

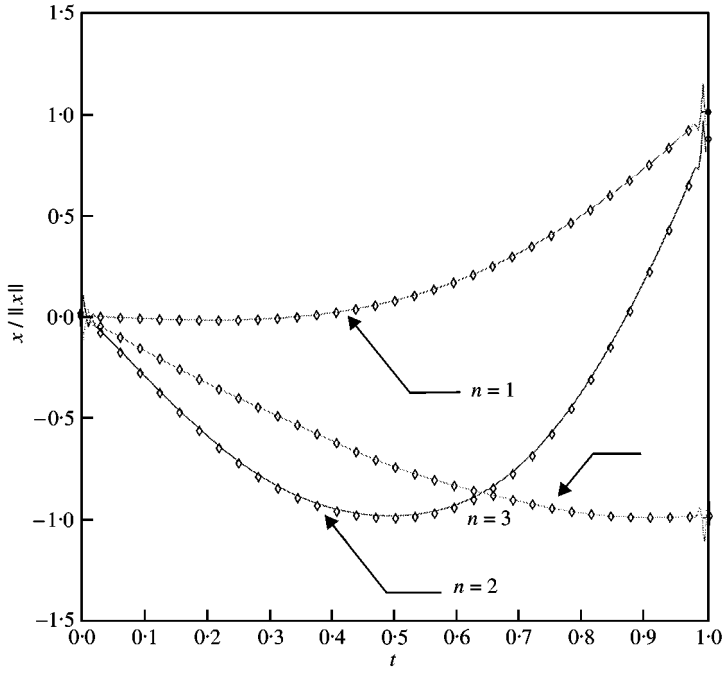

Figure 17. Time responses $[X_n(t)]_{n=1,2,3}$; ◇◇◇◇, RK 45; ——, wavelets.

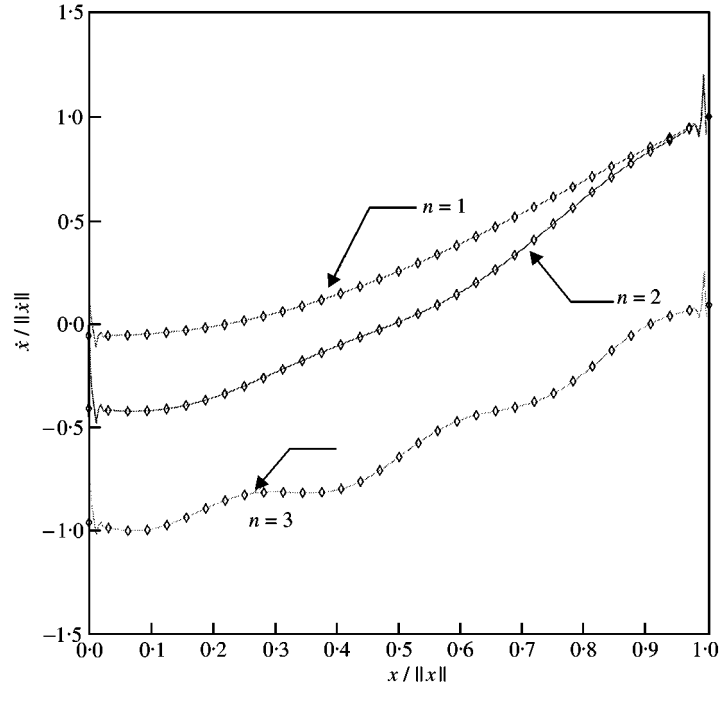

Figure 18. Velocity responses $[\dot{X}_n(t)]_{n=1,2,3}$; ◇◇◇◇, RK 45; ——, wavelets.

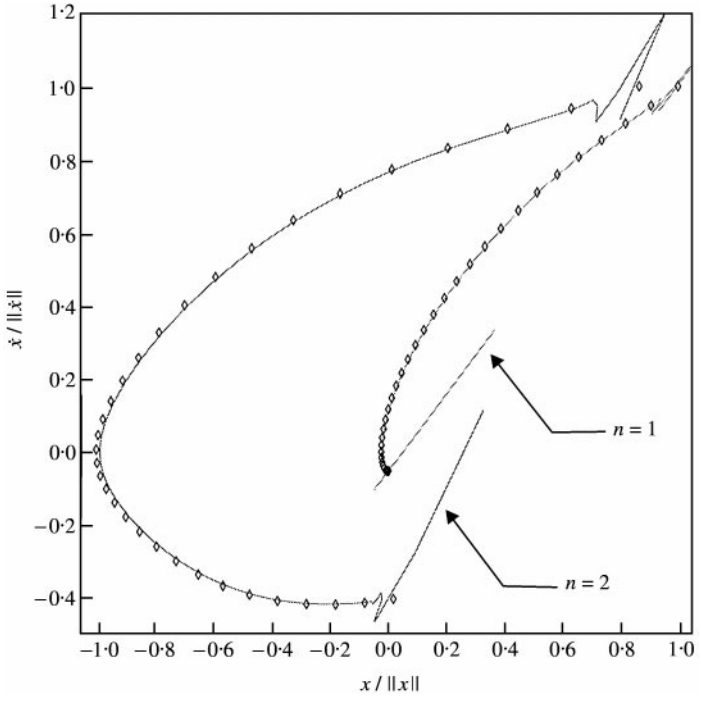

Figure 19. Phase portraits $[X_n/\|X_n\|, \dot{X}_n/\|\dot{X}_n\|]_{n=1,2}$; ◇◇◇◇, RK 45; ——, wavelets.

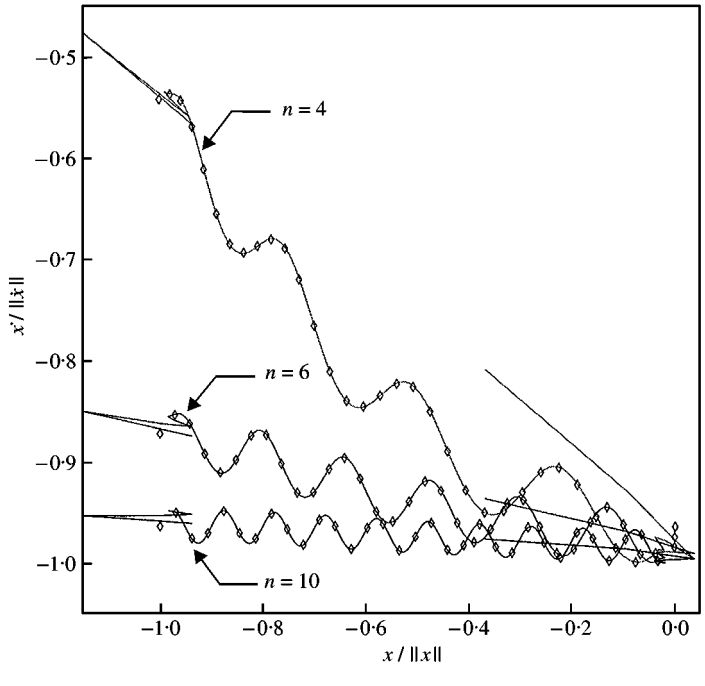

Figure 20. Phase portraits $[X_n/\|X_n\|, \dot{X}_n/\|\dot{X}_n\|]_{n=4,6,10}$; ◇◇◇◇, RK 45; ——, wavelets.

Interesting properties of the wavelet procedure are pointed out: it overcomes problems involving either smooth or very irregular parametric excitations $f_\varepsilon(t)$ as displayed in Figures 8, 11 and 14. Pyramidal wavelet decompositions of signals such as a sinusoid perturbed by a high frequency accident (Figure 9), a transition between a low frequency oscillation and a relatively high frequency oscillation (Figure 12) and an oscillation perturbed by a widespread spectrum noise (Figure 15), are many revealing instances which confirm that the wavelet-Galerkin procedure is able to process experimentally monitored excitations (external or parametric excitations) characterized by a continuous-band spectrum. Moreover, the method appears to be efficient in solving problems involving a relatively large number of d.o.f.: temporal responses (Figures 17 and 18) and phase portraits (Figures 19 and 20) of dynamic components of equation (64) emphasize the reliable behaviour, compared with the Runge–Kutta $RK45$ simulations.
Intrinsic properties may be emphasized:

- the wavelet-Galerkin associated problem may be easily built because it essentially reduces to a pre-computation of the time-scale representations of basic linear operators and a gathering of matrix systems.
- the wavelet method is a multi resolution approach: fast tree algorithms are available to seek finer/coarser wavelet representations of signals/operators,
- the wavelet method gives a functional representation of solutions.

As intrinsic properties highlight both a numerical and an analytical procedure, the wavelet-Galerkin procedure is used in the following section to compute efficiently the Floquet transition matrix involved in a standard stability analysis.

4. STABILITY ANALYSIS: AN EFFICIENT WAVELET PROCEDURE TO COMPUTE THE FLOQUET TRANSITION MATRIX

Focusing on the free oscillation problem (P_s) given by equation (1) and referred to later,

$$(P_s)|\dot{\mathbf{X}}(t) + \boldsymbol{H}_1(t, \boldsymbol{\lambda})\dot{\mathbf{X}}(t) + \boldsymbol{H}_2(t, \boldsymbol{\lambda})\mathbf{X}(t) = \mathbf{0} \quad [\text{Stability}] \tag{66}$$

involving matrices $\boldsymbol{H}_1(t, \boldsymbol{\lambda})$ of $\boldsymbol{H}_2(t, \boldsymbol{\lambda})$ of T-periodic time-varying functions depending on a set of parameters $\boldsymbol{\lambda}$, the following question is raised: in which parameter area is the stability of periodic system P_s guaranteed? Answering that question is relatively straightforward using the theoretical framework of the Floquet theory in reference [1] and briefly referred here to introduce the notations. The general case could be treated, but very often, $\boldsymbol{H}_1(t, \boldsymbol{\lambda})$ is a constant matrix (damping) so that a new variable can be easily introduced (see Liouville's method in reference [2]) $\mathbf{X}(t) = \exp(-(t/2)\boldsymbol{H}_1)\dot{\mathbf{X}}(t)$ in order to obtain

$$\ddot{\tilde{\mathbf{X}}} + \left[\exp\left(-\frac{t}{2}\boldsymbol{H}_1\right)\boldsymbol{H}_2(t, \boldsymbol{\lambda})\exp\left(\frac{t}{2}\boldsymbol{H}_1\right) - \frac{\mathbf{H}_1^2}{4}\right]\tilde{\mathbf{X}}(t) = \mathbf{0}. \tag{67}$$

This last equation explains why the peculiar case

$$\ddot{\mathbf{X}}(t) + \boldsymbol{H}(t, \boldsymbol{\lambda})\mathbf{X}(t) = \mathbf{0} \tag{68}$$

is expecially interesting. This latter case is now the suitable framework considered in the present study.

Condensing time response of P_s and its derivative into $\mathbf{Y} = [\mathbf{X}\ \dot{\mathbf{X}}]^{\mathrm{T}} = [\mathbf{Y}_1\ \mathbf{Y}_2]^{\mathrm{T}}$, the second order differential problem P_s is transformed in a $(2N, 2N)$ first order equivalent system

$$P_s(Y) \left| \begin{bmatrix} \dot{\mathbf{Y}}_1 \\ \dot{\mathbf{Y}}_2 \end{bmatrix} + \begin{bmatrix} \boldsymbol{0}_{(N,N)} & -\boldsymbol{I}_{(N,N)} \\ \boldsymbol{H}(t, \boldsymbol{\lambda}) & \boldsymbol{0}_{(N,N)} \end{bmatrix} \cdot \begin{bmatrix} \mathbf{Y}_1 \\ \mathbf{Y}_2 \end{bmatrix} = \mathbf{0}. \right. \tag{69}$$

The Cauchy theorem claims a fundamental basis of $2N$ solutions $\boldsymbol{\zeta}(t) = [\zeta_1, \ldots, \zeta_{2N}]^{\mathrm{T}}$ of dimension $2N$ exits so that equation

$$[\dot{\boldsymbol{\zeta}}(t)] = \begin{bmatrix} \boldsymbol{0} & -\boldsymbol{I} \\ \boldsymbol{H}(t, \boldsymbol{\lambda}) & \boldsymbol{0} \end{bmatrix} \cdot [\boldsymbol{\zeta}(t)] \tag{70}$$

is confirmed.

At the same time, $\boldsymbol{\zeta}(t + T)$ is also shown to be a fundamental set of solutions using the T-periodicity of $\boldsymbol{H}(t, \boldsymbol{\lambda})$. Consequently, the Floquet theory exhibits a Floquet transition matrix $\boldsymbol{F}$ confirming the relationship

$$[\boldsymbol{\zeta}(t + T)] = [\boldsymbol{F}] \cdot [\boldsymbol{\zeta}(t)]. \tag{71}$$

Hence, it is assumed without restricting the generality that a diagonal form of equation (71) may be computed. Introducing the transformation $\boldsymbol{\zeta}(t) = \boldsymbol{P}\boldsymbol{V}(t)$, it yields

$$\boldsymbol{V}(t + T) = [\boldsymbol{P}^{-1}\boldsymbol{F}\boldsymbol{P}] \cdot \boldsymbol{V}(t) = \begin{bmatrix} \mu_1 & & 0 \\ & \ddots & \\ 0 & & \mu_{2N} \end{bmatrix} \boldsymbol{V}(t), \tag{72}$$

where $(\mu_i)_{1 \leqslant i \leqslant 2N}$ are the eigenvalues of the Floquet transition matrix $\boldsymbol{F}$. Defining the Floquet exponents as $\gamma_i = (1/T) \ln(\mu_i)$, the Floquet theory finally exhibits normal solutions of the form

$$\mathbf{X}_i(t) = \exp(\gamma_i t)\, \boldsymbol{\phi}_i(t) \quad \forall 1 \leqslant i \leqslant 2N \tag{73}$$

with $\boldsymbol{\phi}_i(t) = \boldsymbol{\phi}_i(t + T)$ and γ_i, respectively, standing for periodic solutions and Floquet exponents quantifying stability or instability levels of the system. The following stability criteria are inferred from equation (72):

$$\begin{aligned} &\sup_{1 \leqslant i \leqslant 2N} \mathfrak{Re}(\gamma_i) < 0 \Rightarrow \text{stable system}, \\ &\sup_{1 \leqslant i \leqslant 2N} \mathfrak{Re}(\gamma_i) > 0 \Rightarrow \text{unstable system}, \\ &\sup_{1 \leqslant i \leqslant 2N} \mathfrak{Re}(\gamma_i) = 0 \Rightarrow \text{critical case}. \end{aligned} \tag{74}$$

Summing up, the stability analysis mainly consists of building the Floquet transition matrix $\boldsymbol{F}$ and searching for solutions of equation (70) combined with a set of $2N$ independent initial conditions $\boldsymbol{\zeta}(0) = \boldsymbol{I}_{(N,N)}$ for instance. Using equation (71), the Floquet transition matrix will be identified thanks to the relation $\boldsymbol{F} = \boldsymbol{\zeta}(T)$. Though very robust on the mathematical point of view, the Floquet theory encounters many drawbacks practically. It is often very difficult to obtain the Floquet matrix transition without expensive

computations and in one pass. Here, benefit is made of the wavelet-Galerkin procedure previously described to compute efficiently the Floquet transition matrix in one pass and consequently state according to the stability of the system.

Next, the wavelet procedure is defined to build stability diagrams featuring both qualitative (stability/instability) and quantitative information (strength of stability/instability). Having pre-computed the wavelet "skeleton" of problem P_s:

- solve P_s with $2N$ independent $[\mathbf{X}_0, \dot{\mathbf{X}}_0]$ using the wavelet-Galerkin solver,
- compute the Floquet transition matrix in one pass,
- compute the Floquet exponent whose real part is the highest,
  - state according to the stability criteria: $\Re e(\gamma) < 0$, $\Re e(\gamma) > 0$, $\Re e(\gamma) = 0$,
  - estimate the strength of stability/instability: maximum value of $\Re e(\gamma)$,
- repeat the procedure for each set $\boldsymbol{\lambda}$ ranging in the parameter domain.

This procedure enables a straightforward and very efficient technique to be used to build stability diagrams displaying the isovalue curves of the maximum of the real part of Floquet exponents taking full advantage of the interesting properties of the wavelet-Galerkin solver. It also allows transition curves (qualitative information) to be extracted and the strength of stability/instability (quantitative information) to be measured. The method is used to compute the stability diagram of a Mathieu oscillator and a system of two coupled oscillators with two parameters depicted hereafter.

4.1. STABILITY ANALYSIS OF A s.d.o.f. SYSTEM

The wavelet method is applied (for example) to the Mathieu oscillator [1] depicted by

$$\ddot{x}(t) + (\delta + 2\varepsilon \cos(2t))\, x(t) = 0, \tag{75}$$

where $[\delta, \varepsilon]$ are two intrinsic parameters. On the stability diagram (Figure 21) illustrating a normalized value of the dominant Floquet exponent computed at a resolution scale $J = 8$ (vertically) in terms of parameters δ and ε in horizontal directions, it is noticeable that the transition curves point towards the values $(\delta = n^2)_{n \in \mathbb{Z}}$ which is a well-known result [1]. Yet portions of high instability may be distinguished in the upper left corner of Figure 21 with levels of γ greater than 10. Moreover, the wavelet method allows the strength of stability/instability to be measured thanks to the level of Floquet exponents. In order to demonstrate that the approximation order J has little influence on the shape of stability diagrams as soon as a convenient scale J is used, stability diagrams of the Mathieu oscillator (75) are introduced according to scales J ranging between 3 and 8 as displayed in Figures 21–24. In the present study, convergence is numerically obtained for $J \geqslant 4$ corresponding to an analyzing basis including 16 wavelet patterns.

4.2. STABILITY ANALYSIS OF A TWO d.o.f. SYSTEM

Considering the two d.o.f. system whose motion is governed by equations

$$\begin{aligned} \ddot{x}_1 + a_1\dot{x}_1 + [\delta + 2\varepsilon\cos(2t)]x_1 + 2\varepsilon\cos(2t)x_2 = 0, \\ \ddot{x}_2 + a_2\dot{x}_2 + 2\varepsilon\cos(2t)x_1 + [\delta + 2\varepsilon\cos(2t)]x_2 = 0, \end{aligned} \tag{76}$$

involving the parameters $[\delta, \varepsilon]$ and the viscous damping factors $a_1 = a_2 = 0{\cdot}25$, the corresponding stability diagram is displayed in Figure 25. This diagram was obtained

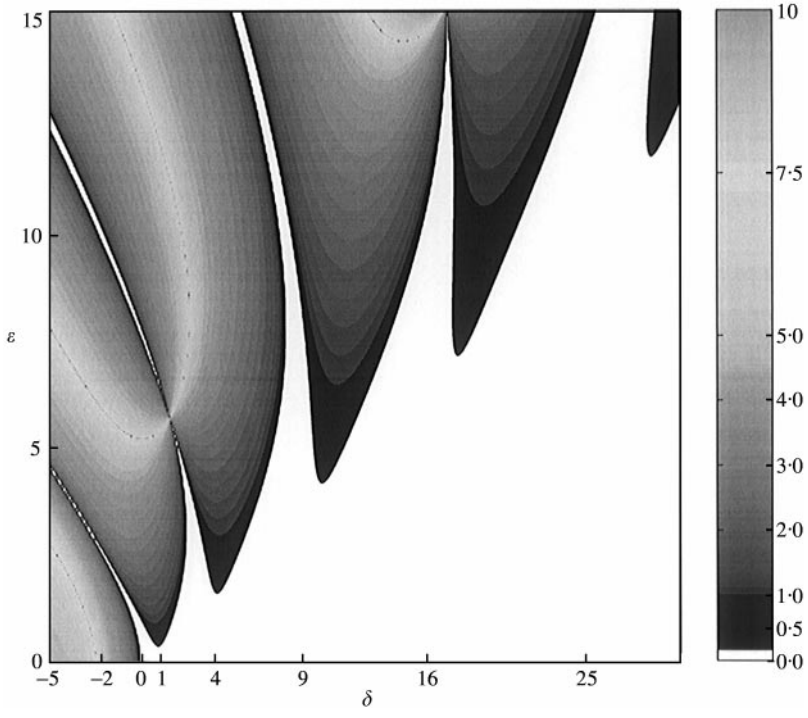

Figure 21. Stability diagram $\|\gamma\| = \mathscr{F}[\delta, \varepsilon]$ of the 1 d.o.f. system with a resolution scale $J = 3$.

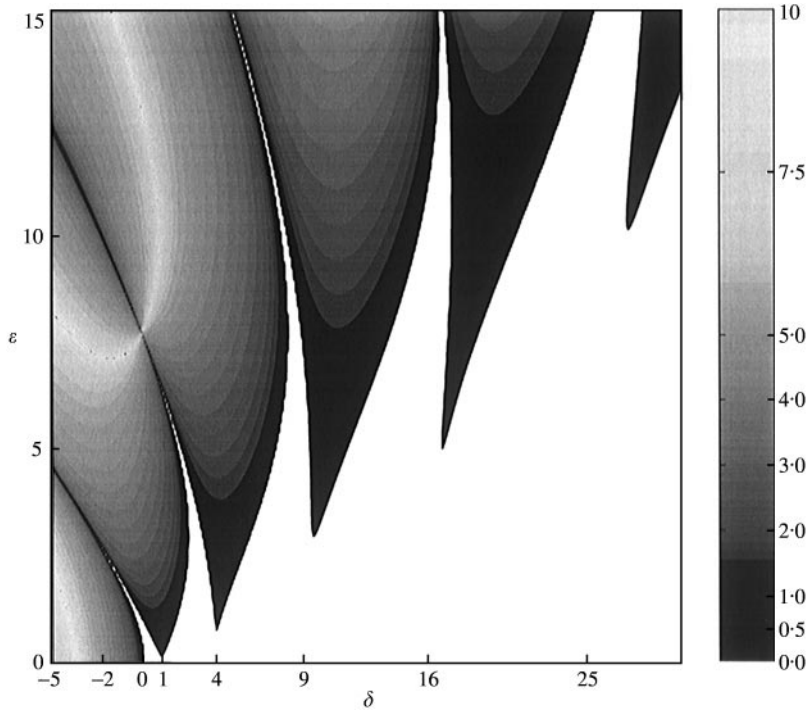

Figure 22. Stability diagram $\|\gamma\| = \mathscr{F}[\delta, \varepsilon]$ of the 1 d.o.f. system with a resolution scale $J = 4$.

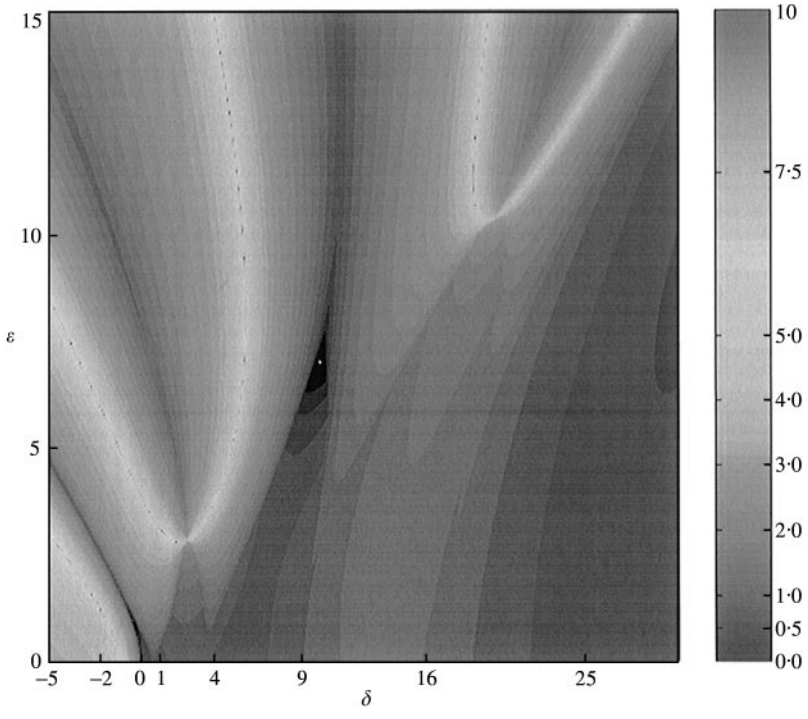

Figure 23. Stability diagram $\|\gamma\| = \mathscr{F}[\delta, \varepsilon]$ of the 1 d.o.f. system with a resolution scale $J = 6$.

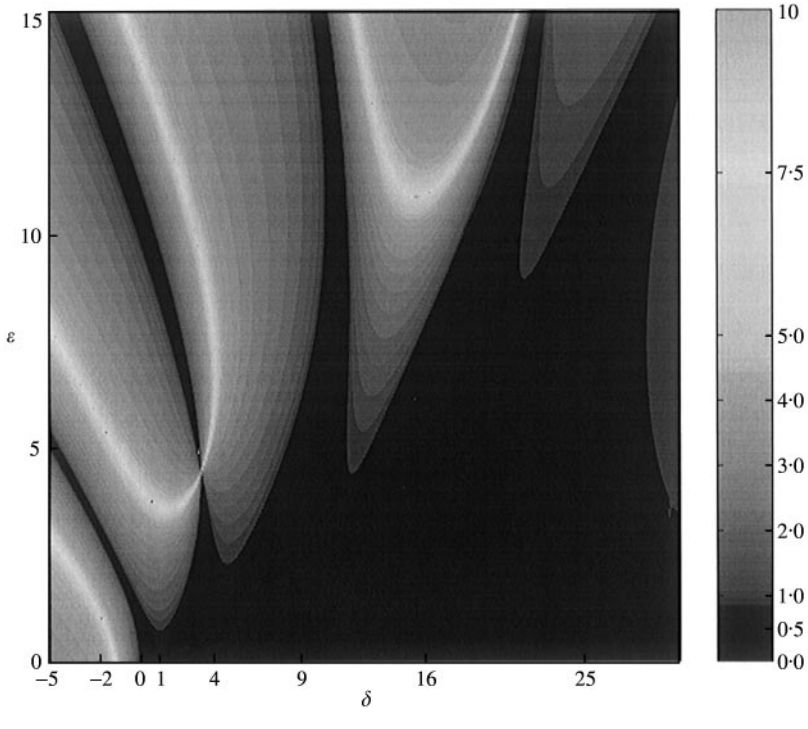

Figure 24. Stability diagram $\|\gamma\| = \mathscr{F}[\delta, \varepsilon]$ of the 1 d.o.f. system with a resolution scale $J = 8$.

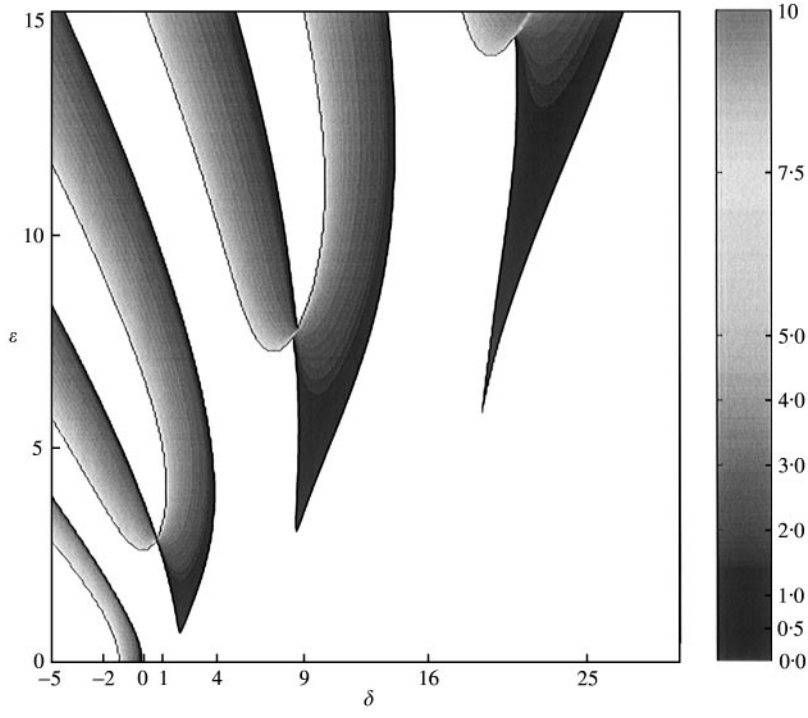

Figure 25. Stability diagram $\|\gamma\| = \mathscr{F}[\delta, \varepsilon]$ of the 2 d.o.f. system with a resolution scale $J = 6$.

without any major difficulty as in the one d.o.f. case. Compared with the stability diagrams of the single d.o.f. Mathieu oscillator (75), several stable band areas are noticeable (for instance, in the neighbourhood of $\delta \simeq 9$). Independently of the damping that shifts the stability diagram up, it can be claimed that the presence of two oscillators has a stabilizing effect on both and consequently plays a great part in the stability of the whole system (76) by spreading the stable areas, as expected.

5. CONCLUSION

A new wavelet-Galerkin procedure was introduced to investigate transient vibration and stability of parametrically excited systems and more generally time-periodic systems. The multi-scale method proved to be reliable for systems involving irregular excitations, with a relatively high number of d.o.f. by comparison with a standard integration procedure of Runge–Kutta type, as illustrated in the academic instances. Having stored time-scale representation of a few elementary operators in wavelet bases, stability diagrams can easily be produced exhibiting the transition curves and the Floquet exponents giving a quantization of stability/instability levels can be estimated.

The new wavelet-based procedure is very promising and permits the linearized stability of non-linear systems to be investigated. A brief comparison may be established with some other classical methods: among other existing numerical or analytical methods such as continuation, multiple scales, normal form or Chebyshev–Galerkin, the wavelet-Galerkin procedure may be viewed both as a numerical and an analytical method. On the one hand, numerical methods based on a continuation procedure cannot provide a quantization of stability when the problem of concern is to compute the transitions between stable and

unstable areas (bound to periodic solutions). These methods are computationally very time-consuming for they require calculations for each set of parameters and time-accidents in solutions to be captured using small time steps for localized stiffness. On the other hand, analytical methods only proved their efficiency for a few degrees of freedom (1, 2, perhaps 3), practically speaking. They provide interesting algebraic equations, but still they remain only approximated methods when dealing with problems involving strong non-linearities of strong parametric excitations. Consequently, it is often impossible to quantify error levels that might be large. The wavelet-Galerkin method is conceptually close to the Chebyschev-Galerkin method described by Sinha in reference [23] but it takes advantage of the wavelet properties (fairly good time–frequency localization, fast trees algorithms, non-standard form and compression of operators in wavelet bases) that are not available using polynomial bases. Moreover, because the wavelet method can provide both transient and periodic solutions using the same tools, quantization of stability is worthy and relatively straightforward.

In the present study, only transient responses were investigated using the wavelet-Galerkin solver. A further paper in progress (a wavelet-based procedure to find periodic orbits of parametrically excited systems' by C. H. Lamarque and S. Pernot), will focus on the search of (stationary) periodic responses of system P and their corresponding periodic initial conditions $(\mathbf{X}_0^{per}, \dot{\mathbf{X}}_0^{per})$. At the present time, interesting multi-scale properties have not been fully exploited and future prospects concern the development of a new wavelet-balance procedure allowing a real time-scale representation of vibrations of any non-linear dynamical system adopting a multi-resolution approach of the underlying phenomena. This wavelet-balance method is described in 'a wavelet-balance method to investigate the vibrations of nonlinear dynamical systems' (S. Pernot and C. H. Lamarque) to be submitted for publication.

REFERENCES

1. A. H. Nayfeh and D. T. Mook 1979 *Nonlinear Oscillations*. New York: Wiley.
2. P. Hartman 1982 *Ordinary Differential Equations*. Boston, Basel, Stuttgart: Birkhaüser; second edition, reprint.
3. J. L. Willems 1970 *Stability Theory of Dynamical Systems*. London: Nelson.
4. L. Meirovitch 1967 *Analytical Methods in Vibrations*. London: MacMillan.
5. A. H. Nayfeh 1973 *Perturbation Methods*. New York: Wiley & Sons.
6. G. E. Giacaglia 1972 *Perturbation Methods in Nonlinear Systems*, Vol. 8. Applied Mathematical Science. Berlin: Springer.
7. A. D. Brjuno 1989 *Local Methods in Nonlinear Differential Equations*. New York: Springer.
8. V. I. Arnold 1980 *Chapitres supplémentaires à la théorie des équations différentielles ordinaires*. Moscou: Editions de Moscou.
9. G. Iooss and D. D. Joseph 1980 *Elementary Bifurcation and Stability Theory*. New York, Berlin, Heidelberg: Springer.
10. G. Iooss and M. Adelmeyer 1992 *Topics in Bifurcation Theory and Applications*, Advanced Series in Nonlinear Dynamics. Vol. 3. Singapore: World Scientific.
11. L. Hsu 1993 *Journal of Sound and Vibrations*. **89**, 169–182. Analysis of critical and post-critical behavior of nonlinear dynamical systems by the normal form method-Part I. Normalization formulae.
12. A. H. Nayfeh 1993 *Method of Normal Forms*. New York: Wiley.
13. H. L. Smith 1986 *Journal of Mathematical Analysis and Applications* **113**, 578–560. Normal forms for periodic systems.
14. L. Jezequel and C. H. Lamarque 1991 *Journal of Sound and Vibrations* **149**, 429–459. Analysis of nonlinear structural vibrations by normal form theory.
15. C. S Hsu 1963 *American Society of Mechanical Engineers Journal of Applied Mechanics* **30**, 367–372. On the parametric excitation of a dynamic system having multiple degrees of freedom.

16. N. N. BOGOLIUBOV and Y. A. MITROPOLSKI 1961 *Asymptotic Methods in the Theory of Nonlinear Oscillations*. New York: Gordon and Breach.
17. M. ROSEAU 1996 *Vibrations des systèmes mécaniques, méthodes analytiques et applications*. Paris: Masson.
18. F. VERHULST 1996 *Nonlinear Differential Equations and Dynamical Systems*. Berlin: Springer Verlag.
19. V. V. BOLOTIN 1963 *Nonconservative Problems of the Theory of Elastic Stability*. New York: Pergamon Press.
20. K. TAKAHASHI 1981 *Journal of Sound and Vibration* **78**, 519–529. An approach to investigate parametric dynamic systems.
21. Ö. TURHAN 1998 *Journal of Sound and Vibration* **216**, 851–863. A generalized Bolotin's method for stability limit determination of parametrically excited systems.
22. R. S. GUTTALU and H. FLASHNER 1996 *Journal of Sound and Vibration* **189**, 33–54. Stability analysis of periodic systems by truncated point mappings.
23. S. C. SINHA and D. H. WU 1991 *Journal of Sound and Vibration* **151**, 91–117. An efficient computational scheme for the analysis of periodic systems.
24. S. C. SINHA, E. A. BUTCHER and A. DAVID 1998 *Nonlinear Dynamics* **16**, 203–221. Construction of dynamically equivalent time-invariant forms for time-periodic systems.
25. E. I. ALLGOWER and K. GEORG 1990 *SCM* **13**, *Numerical Continuation Methods*. Berlin: Springer-Verlag.
26. C.-H. LAMARQUE and A. STOFFEL 1992 *Mechanics Research Communications* **19**, 495–504. Parametric resonance with a nonlinear term: comparison of averaging and the normal form method using a simple example.
27. I. DAUBECHIES 1988 *Communications on Pure and Applied Mathematics* **XLI**, 909–996. Orthonormal bases of compactly supported wavelets.
28. V. PERRIER and C. BASDEVANT 1989 *La recherche aérospatiale* **3**, 53–67. La décomposition en ondelettes périodiques, un outil pour l'analyse de champs inhomogènes: théorie et algorithmes, mai–juin.
29. S. MALLAT 1989 *IEEE Transactions on Pattern Analysis and Machine Intelligence* **11**, 674–693. A theory for multiresolution signal decomposition: the wavelet representation.
30. Y. MEYER 1990 *Ondelettes et Operareurs I*, *Ondelettes*. Actualités mathématiques. Paris: Hermann.
31. I. DAUBECHIES 1992 *Ten lectures on Wavelets*, *CBMS Lecture Notes*, Vol. 61. Philadelphia, PA: SIAM.
32. W. SWELDENS 1995 *Ph.D. Thesis*, *University of South Carolina*. The construction and application of wavelets in numerical analysis.
33. A. COHEN and A. EZZINE 1996 *Comptes-Rendus de l'Académie des Sciences de Paris* t. **323**, 829–834. Quadratures singulières et fonctions d'échelle.
34. G. BEYLKIN, R. COIFMAN and V. ROKHLIN 1991 *Communications on Pure and Applied Mathematics* XLIV, 141–183. Fast wavelet transforms and numerical algorithms I, Yale University.
35. G. BEYLKIN 1992 *SIAM Journal on Numerical Analysis* **29**, 1716–1740. On the representation of operators in bases of compactly supported wavelets.
36. S. PERNOT 2000 *Ph.D. Thesis in Civil Engineering*, *Institut National des Sciences Appliquées*, *Lyon*, *France*, ISAL no. 0071. 441 pages. Méthodes Ondelettes pour l'Etude des Vibrations et de la Stabilité des Systèmes Dynamiques.
37. M. Q. CHEN, C. HWANG and Y. P. SHIH 1996 *International Journal for Numerical Methods in Engineering* **39**, 2921–2944. The computation of wavelet-Galerkin approximation on a bounded interval.
38. D. L. GINES, G. BEYLKIN and J. DUNN 1996 *Technical report*, *University of Colorado*, *Boulder*, *PAM. Report*. LU factorization of non-standard forms and direct multiresolution solvers.